Bed nucleus of the stria terminalis regulates fear to unpredictable threat signals

Travis D. Goode[1], Reed L. Ressler[1], Gillian M. Acca[1], Olivia W. Miles[1], Stephen Maren[1,2]

[1]*Department of Psychological and Brain Sciences and Institute for Neuroscience, Texas A&M University, College Station, TX, 77843-3474, USA*

[2]*Corresponding author*

Email:	maren@tamu.edu
Phone:	979-458-7960
Address:	Stephen Maren Department of Psychological and Brain Sciences Texas A&M University 301 Old Main Dr. College Station, TX 77843-3474

ORCiD

Travis D. Goode:	https://orcid.org/0000-0003-1432-8894
Reed L. Ressler:	https://orcid.org/0000-0003-0514-8269
Olivia W. Miles:	https://orcid.org/0000-0001-9422-8855
Stephen Maren:	https://orcid.org/0000-0002-9342-7411

ABSTRACT

The bed nucleus of the stria terminalis (BNST) has been implicated in conditioned fear and anxiety, but the specific factors that engage the BNST in defensive behaviors are unclear. Here we examined whether the BNST mediates freezing to conditioned stimuli (CSs) that poorly predict the onset of aversive unconditioned stimuli (USs) in rats. Reversible inactivation of the BNST selectively reduced freezing to CSs that poorly signaled US onset (e.g., a backward CS that followed the US), but did not eliminate freezing to forward CSs even when they predicted USs of variable intensity. Additionally, backward (but not forward) CSs selectively increased Fos in the ventral BNST and in BNST-projecting neurons in the infralimbic region of the medial prefrontal cortex (mPFC), but not in the hippocampus or amygdala. These data reveal that BNST circuits regulate fear to unpredictable threats, which may be critical to the etiology and expression of anxiety.

IMPACT STATEMENT

The bed nucleus of the stria terminalis (BNST) is required for the expression of defensive behavior to unpredictable threats, a function that may be central to pathological anxiety.

INTRODUCTION

Excessive apprehension about potential future threats, including financial loss, illness, or death, is a defining feature of many anxiety disorders, including generalized anxiety disorder (GAD) (Behar et al., 2009). Anxiety and trauma-related disorders are widespread and costly (Blanco et al., 2011; Comer et al., 2011; Kinley et al., 2011; Salas-Wright et al., 2014; Stein et al., 2017; Wittchen, 2002), and remain difficult to treat (Colvonen et al., 2017; Costello et al., 2014; Iza et al., 2013; Sinnema et al., 2015). Understanding the neural circuits underlying anxiety is important for refining behavioral and pharmacotherapeutic treatments (Berridge, 2018; Deslauriers et al., 2017; Fanselow and Pennington, 2018, 2017; Graham et al., 2014; LeDoux and Daw, 2018; Nees et al., 2015; Pine and LeDoux, 2017; Tye, 2018). Several recent studies have demonstrated changes in the function of the bed nucleus of the stria terminalis (BNST) in individuals with post-traumatic stress disorder (PTSD) and anxiety disorders (Andreescu et al., 2015; Brinkmann et al., 2018; L Brinkmann et al., 2017; Leonie Brinkmann et al., 2017; Buff et al., 2017; Münsterkötter et al., 2015; Rabellino et al., 2018; Straube et al., 2007; Yassa et al., 2012). However, the conditions that recruit the BNST to aversive learning and memory processes believed to underlie anxiety disorders are still not understood (Avery et al., 2016, 2014; Ch'ng et al., 2018; Daniel and Rainnie, 2016; Davis et al., 2010; Fox and Shackman, 2017; Goode and Maren, 2017; Gungor and Paré, 2016; Lebow and Chen, 2016; Perusini and Fanselow, 2015; Shackman and Fox, 2016; Walker et al., 2009; Walker and Davis, 2008).

Early work on this question revealed that BNST lesions in rats impair defensive behaviors evoked by unconditioned threats (Gewirtz et al., 1998). For example, BNST inactivation results in a loss of unconditioned defensive responding to the presence of predator odors (Breitfeld et al.,

2015; Fendt et al., 2003; Xu et al., 2012). Additionally, unconditioned increases in the acoustic startle reflex produced by either intracranial administration of corticotropin-releasing factor (CRF) or exposure to bright light require the BNST, whereas fear-potentiated startle to punctate conditioned stimuli (CSs) do not (Walker et al., 2009). However, the involvement of the BNST in defensive responding is not restricted to unconditioned threat: BNST lesions produce deficits in both freezing and corticosterone release elicited by contextual, but not auditory, CSs after Pavlovian fear conditioning in rats (LeDoux et al., 1988; Sullivan et al., 2004). Interestingly, however, it is not stimulus modality that differentiates the effects of BNST lesions on tone and context freezing. BNST lesions impair freezing responses to long-duration (e.g., 10-min) auditory conditioned stimuli (CSs) (Waddell et al., 2006), and spare freezing to short-duration (1-min) contextual stimuli (Hammack et al., 2015). Based on this work, it has been proposed that the BNST is required to organize behavioral and hormonal responses to sustained threats (whether conditioned or unconditioned) (Hammack et al., 2015, 2009; Takahashi, 2014; Waddell et al., 2008, 2006). Of course, the duration of the behavioral responses in these situations is confounded with the duration of the eliciting stimulus. Thus, it has been argued that the BNST mediates sustained defensive *responses* independent of the specific features and durations of the stimuli that evoke them (Davis, 2006; Davis et al., 2010; Walker et al., 2009; Walker and Davis, 2008).

Of course, another factor that differentiates discrete tones from contexts, or short- from long-duration stimuli (whether tones or contexts), is the temporal information the stimuli provide about when an aversive event will occur (Goode and Maren, 2017). For example, long-duration CSs or contexts provide relatively poor information about *when* a future US will occur (i.e., the US will occur at some distal time in the future), whereas short-duration CSs or contexts provide more immediate certainty about the temporal imminence of US onset (i.e., the US will occur soon).

47 We and others have proposed that the BNST may have a critical role in processing temporally
48 unpredictable threats, particularly in mediating defensive responses to threatening stimuli that
49 poorly predict when an aversive event will occur (Goode and Maren, 2017; Lange et al., 2017;
50 Luyck et al., 2018a). Consistent with this view, punctate auditory CSs that are followed by shock
51 at unpredictable latencies yield freezing responses that are sensitive to BNST manipulations
52 (Daldrup et al., 2016; Lange et al., 2017). This suggests that a crucial parameter that determines
53 the role for the BNST in defensive behavior is neither the duration nor modality of the threat (nor
54 the duration of the elicited defensive response), but rather the information a signal provides about
55 when an aversive event will occur.

56 Here we directly examined this possibility by investigating the role of the BNST in
57 conditioned freezing responses elicited by procedures that equated both the duration and modality
58 of the threat CSs, as well as the total number of unconditioned stimulus (US) presentations, but
59 differed according to the timing of the aversive US in relation to the CS. Specifically, we arranged
60 a brief (10-sec) auditory CS to either precede (forward conditioning, FW) or follow (backward
61 conditioning, BW) a footshock US in rats. Although extensively-trained BW CSs become
62 conditioned inhibitors that dampen responding to other first-order excitatory cues (Andreatta et
63 al., 2012; Ayres et al., 1976; Christianson et al., 2011; Gerber et al., 2014; Moscovitch and
64 LoLordo, 1968; Siegel and Domjan, 1971), minimally-trained BW CSs elicit excitatory
65 conditioned responses that transfer across contexts (Ayres et al., 1987; Barnet and Miller, 1996;
66 Bevins and Ayres, 1992; Chang et al., 2003; Connor et al., 2017; Heth, 1976; Mahoney and Ayres,
67 1976; Prével et al., 2018, 2016; Rescorla, 1968). After conditioning, we examined the effect of
68 pharmacological inactivation of the BNST on freezing to FW or BW CSs. We hypothesized that
69 pharmacological inactivation of the BNST would selectively disrupt fear expression to the BW CS

70 and that the presentation of the BW CS would recruit BNST neurons (as assessed by Fos) in greater
71 numbers than the FW CS. Furthermore, we anticipated that the backward CS would increase the
72 activity of BNST-projecting neurons in afferent brain regions implicated in anxiety states.
73 Consistent with our hypothesis, we found that BNST inactivation reduced freezing to a BW, but
74 not FW, CS. This effect was related to the uncertainty of the BW CS in predicting US onset,
75 because the same outcome was observed when USs occurred randomly with respect to the CS. We
76 also observed that BW CSs selectively increased Fos expression in the BNST and BNST-
77 projecting medial prefrontal cortical (mPFC) neurons. These data reveal that BNST circuits
78 process the expression of defensive behavior in the presence of unpredictable threat signals.
79
80 **RESULTS**
81
82 ***Reversible inactivation of the BNST attenuates fear to backward, not forward, CSs.*** To examine
83 the role of the BNST in threat uncertainty, we reversibly inactivated the BNST during retrieval of
84 fear to either a forward- ("FW"; predictable threat) or backward-trained ("BW"; unpredictable
85 threat) CS. A schematic of the behavioral design is shown in Figure 1A. Representative cannula
86 tracts and histological placements are presented in Figure 1—Figure Supplement 1 and Figure 1—
87 Figure Supplement 2 (respectively). Freezing behavior during the conditioning session is shown
88 in Figure 1B. A main effect of conditioning trial was observed (repeated measures: $F_{6,288} = 37.87$,
89 $p < 0.0001$). No other significant main effects or interactions were observed for any of the
90 conditioning or drug assignments across the conditioning trials (F's < 0.70, p's > 0.60).
91 One day after conditioning, the animals were infused with NBQX, an AMPA receptor
92 antagonist, to reversibly inactivate the BNST; saline ("VEH") infusions served as a control.

Immediately after the infusions, the rats were placed in a novel context and received twelve presentations of the CS [some BW-trained rats received no CS exposure at the test, "NoCS(Test)"]. As shown in (Figure 1B), inactivation of the BNST produced a selective decrease in conditioned freezing to the BW CS. Analysis of freezing behavior across the entire session (including the baseline) revealed a main effect of trial (repeated measures: $F_{6,264} = 8.06$, $p < 0.0001$), a significant main effect of CS exposure ($F_{2,44} = 25.38$, $p < 0.0001$), and a significant CS × drug interaction ($F_{2,44} = 3.66$, $p < 0.05$). There were no other main effects or interactions (F's < 1.6, p's > 0.05). Fisher's PLSD indicated that rats in the FW condition exhibited significantly more freezing during the retrieval test than rats in all other groups (p's < 0.05). BW-VEH rats exhibited significantly higher levels of freezing than BW-NBQX rats ($p < 0.005$); BW-NBQX rats did not significantly differ from the NoCS(Test) groups.

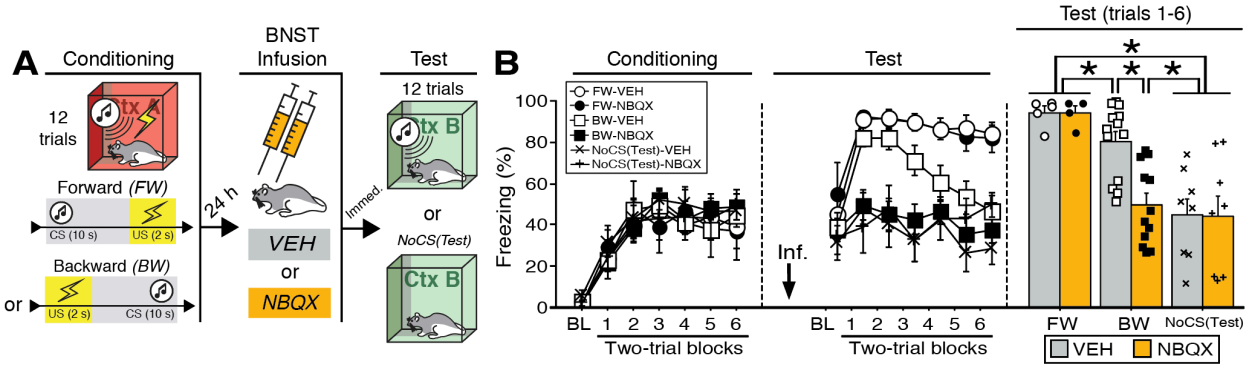

Figure 1. *Reversible inactivation of the BNST attenuates conditioned fear expression to a backward, but not forward, CS.* **(A)** Behavioral schematic. **(B)** Freezing behavior at conditioning and retrieval testing. For conditioning, the left panel depicts mean percentage freezing during the 5-min baseline (BL) and across each conditioning block (each 138-sec block is comprised of two trials; conditioning trials consist of freezing during the 10-sec CS followed by the 58-sec interstimulus interval). For retrieval testing, the center panel shows mean percentage freezing at the 5-min baseline (BL) and across each test block (each 140-sec block is comprised of two trials; trials consist of freezing during the 10-sec CS followed by the 60-sec interstimulus interval). The right panel shows mean percentage freezing during the first half of the test (trials 1-6; corresponding to 420 sec of behavior). All data are represented as means ± s.e.m [FW-VEH (n = 5); FW-NBQX (n = 4); BW-VEH (n = 13); BW-NBQX (n = 12); NoCS(Test)-VEH (n = 8); NoCS(Test)-NBQX (n = 8)]; * = $p < 0.05$.

104 Given that freezing to the BW CS in the VEH-treated animals was maximal in the first half
105 of the test, a separate factorial ANOVA was performed on the average percentage of freezing
106 during trials 1-6 (Figure 1B). For this period, there was a main effect of CS treatment ($F_{2,44}$ =
107 18.61, $p < 0.0001$) as well as a CS treatment × drug interaction ($F_{2,44} = 3.81$, $p < 0.05$); there was
108 no main effect of drug across all groups ($F < 3.00$, $p > 0.05$). Fisher's PLSD revealed significant
109 differences in NBQX- and VEH-treated animals in the BW group ($p < 0.0005$). Additionally, rats
110 in the NoCS(Test) groups differed from all others (p's < 0.0005) except those in the BW-NBQX
111 group, indicating selective reduction of CS-elicited freezing in the BW-NBQX animals. It has been
112 suggested that the BNST mediates sustained but not acute fear responses (Davis, 2006; Davis et
113 al., 2010; Walker et al., 2009; Walker and Davis, 2008). However, it is notable that in this
114 experiment BNST inactivation selectively attenuated conditioned freezing to the backward CS,
115 which produced less sustained freezing during the retrieval test compared to the FW CS.

116 The different effects of BNST inactivation on freezing to FW and BW CSs may have been
117 related to differences in memory strength between the two CSs (reflected in overall levels of
118 freezing to each CS across the retrieval test). Indeed, to generate conditioned freezing to a
119 backward CS we used more conditioning trials than typical in our laboratory. Of course, this may
120 have resulted in moderate overtraining of the FW CS, which might have rendered the FW response
121 less sensitive to disruption. To examine this possibility, we also examined the effects of BNST
122 inactivation of FW and BW conditioning after five conditioning trials (Figure 1—Figure
123 Supplement 3). The behavioral design for the five-trial experiment is shown in Figure 1—Figure
124 Supplement 3A; cannula placements for this experiment are shown in Figure 1—Figure
125 Supplement 4.

126 During the 5-trial conditioning procedure (Figure 1—Figure Supplement 3B), animals
127 exhibited reliable increases in freezing across the session (repeated measures: $F_{5,115} = 12.154$, $p <$
128 0.0001; there were no main effects of conditioning procedure or drug treatment and no interaction
129 of these variables: F's < 2.3, p's > 0.15). After infusions of NBQX or VEH, animals were tested
130 to the CS in a familiar context that was distinct from the conditioning context. As shown in Figure
131 1—Figure Supplement 3B, BNST inactivation did not affect conditioned freezing to either the FW
132 or BW CS. An ANOVA revealed a main effect of trial (repeated measures [including baseline
133 freezing]: $F_{5,105} = 22.118$, $p < 0.0001$), a main effect of conditioning procedure ($F_{1,21} = 15.930$, p
134 < 0.001), and a trial × conditioning procedure interaction (repeated measures: $F_{5,105} = 12.346$, $p <$
135 0.0001). A separate ANOVA performed on trials 1-5 (excluding baseline; Figure 1—Figure
136 Supplement 3B) revealed a significant main effect of conditioning procedure ($F_{1,21} = 21.585$, $p =$
137 0.0001; there was no main effect of drug and no interaction: F's < 0.15, p's > 0.7). Thus, the failure
138 of BNST inactivation to impair conditioned freezing to the FW CS in the 12-trial procedure does
139 not appear to be due to a ceiling effect; freezing to the FW CS in the 5-trial procedure was not
140 maximal and remained insensitive to BNST inactivation. That said, the absence of an effect of
141 BNST inactivation on freezing to the BW CS in this experiment may be due to a floor effect insofar
142 as the 5-trial procedure did not yield conditional significant freezing to the CS (at least freezing
143 that exceeded the pre-CS baseline). Together, these data indicate that the BNST is required for the
144 expression of conditioned freezing to an excitatory BW, but not FW, CS.

145 One index that might reveal differences in the ability of the CS to predict the US is the US-
146 evoked response itself. Footshock USs elicit an unconditioned response (UR) that includes
147 vocalization, autonomic adjustments, and burst of locomotor activity (Bali and Jaggi, 2015;
148 Fanselow, 1994). To better understand the mechanisms of forward and backward conditioning on

149 behavior, we examined shock-evoked activity bursts (Kunwar et al., 2015; Zelikowsky et al., 2018)
150 during the conditioning session in a separate cohort of animals (Figure 1—Figure Supplement 5).
151 Fear conditioning resulted in robust freezing in both groups of animals (Figure 1—Figure
152 Supplement 5A). An ANOVA revealed a significant main effect of trial (repeated measures: $F_{6,180}$
153 $= 67.02$, $p < 0.0001$) with no differences between levels of freezing in FW or BW animals (no
154 other main effects and no interactions: F's < 1.80, p's > 0.15). In contrast, shock-induced activity
155 differed in FW and BW animals (Figure 1—Figure Supplement 5C). All animals exhibited a
156 reliable decrease in shock-induced activity across the conditioning session ($F_{5,150} = 9.59$, $p <$
157 0.0001) and the rate of decline in activity was similar in the two groups (no trial × group
158 interaction: $F < 1.70$, $p > 0.09$), but the overall level of shock-induced activity was significantly
159 lower in the FW animals (main effect of group: $F_{1,30} = 9.59$, $p < 0.05$). For comparison, two-tailed
160 unpaired t-test of mean levels of activity during the 5-min baseline revealed no significant
161 difference between FW and BW rats (Figure 1—Figure Supplement 5B; $t < 0.30$; $p > 0.75$). Hence,
162 USs that were not signaled by a forward CS evoked greater activity bursts than those that were,
163 which may suggest greater regulation of the shock-induced activity when the US is preceded by a
164 temporally predictive cue.
165
166 ***Inactivation of the BNST disrupts freezing to a discrete CS associated with random USs.*** The
167 differential effect of BNST inactivation on freezing to a FW or BW CS suggests that the BNST
168 regulates defensive behavior to stimuli that poorly signal US onset. However, the BW CS does not
169 completely lack temporal information about US onset; the BW conditioning procedure may have
170 resulted in forward trace conditioning to the CS, which always preceded the next US by 60-sec
171 (after trial 1). To address this possibility, separate rats were implanted with cannulas in the BNST
172 and submitted to one of three conditioning procedures (Figure 2). In the first group, animals were

173 conditioned to a backward CS (identical to 12-trial experiment above; "BW"). In the second group,
174 animals received CS presentations followed by randomized onset of the US ("RANDOM"). In the
175 third control group, animals were conditioned using the RANDOM procedure but in the absence
176 of any CS ["NoCS(Cond)"]. A summary of the behavioral design is shown in Figure 2A [the
177 $GABA_A$ receptor agonist muscimol ("MUS") was used to reversibly inactivate the BNST in this
178 and subsequent experiments; see Materials and Methods]. Cannula placements for these animals
179 are shown in Fig. 2—Figure Supplement 1.

180 The percentage of freezing during fear conditioning for the RANDOM, BW, and
181 NoCS(Cond) procedures is shown in Figure 2B. For conditioning, an ANOVA revealed a main
182 effect of trial (repeated measures: $F_{6,204} = 85.209$, $p < 0.0001$), insofar as all groups reliably
183 increased their freezing across the conditioning trials. There was no main effect of conditioning
184 procedure ($F < 3.10$, $p > 0.05$) and no main effect or interactions with regards to future drug or
185 vehicle assignments (F's < 1.00, p's > 0.30).

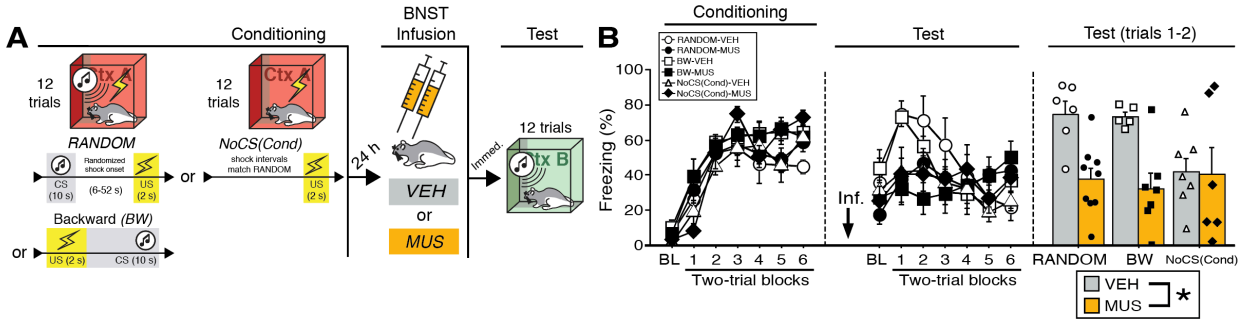

Figure 2. *BNST inactivation attenuates freezing to a discrete CS paired with random onset of shock.* **(A)** Behavioral schematic. **(B)** Freezing behavior during conditioning and retrieval testing. For conditioning, the left panel depicts mean percentage freezing during the 5-min baseline (BL) and across each conditioning block (each block is comprised of two trials; trials consist of freezing during the 10-sec CS followed by the 58-sec interval for the BW animals, whereas blocks for the other groups include equivalent time periods which include the CS [if present] and inter-CS intervals [excluding the duration of the shock]). For retrieval testing, the center panel shows mean percentage freezing at the 5-min baseline (BL) and across each test block (each 140-sec block is comprised of two trials; trials consist of freezing during the 10-sec CS followed by the 60-sec interval). The right panel shows mean percentage freezing across the first two test trials (after BL; corresponding to 140 sec of behavior). All data are represented as means ± s.e.m [RANDOM-VEH (n = 6); RANDOM-MUS (n = 9); BW-VEH (n = 5); BW-MUS (n = 7); NoCS(Cond)-VEH (n = 7); NoCS(Cond)-VEH (n = 6)].

186 As shown in Figure 2B, inactivation of the BNST produced deficits in freezing during
187 retrieval testing in the BW and RANDOM groups, but did not affect freezing in the NoCS(Cond)
188 control. This was confirmed in an ANOVA that revealed a significant drug × trial interaction
189 (repeated measures: $F_{6,204} = 7.91$, $p < 0.0001$). A significant main effect of trial (repeated measures:
190 $F_{6,204} = 7.80$, $p < 0.0001$) indicated significant changes in freezing across the entire test amongst
191 all groups. No other significant main effects or interactions were detected for this test (F's < 1.80,
192 p's > 0.05). Similar to the aforementioned experiments, freezing was maximal in the early test
193 trials, so a separate ANOVA was performed on mean responding during the first two trials of
194 testing (Figure 2B). These analyses revealed a significant main effect of drug ($F_{1,34} = 12.82$, $p <$
195 0.005), indicating a disruption of freezing in drug-treated animals; no other significant main effects
196 or interactions were detected for these trials (F's < 3.00, p's > 0.07). Similar results were obtained
197 if the ANOVA was restricted to the first six trials of the test (main effect of drug: $F_{1,34} = 6.217$, p
198 < 0.05; no other significant main effects or interactions, F's < 1.90, p's > 0.16). Excluding
199 NoCS(Cond) animals, a main effect of drug treatment was also identified for the first two-trial
200 block of the test ($F_{1,23} = 28.115$, $p < 0.0001$). Additionally, we ran an ANOVA solely on baseline
201 freezing. MUS-treated animals exhibited a trending, but nonsignificant ($F < 4.1$, $p > 0.05$),
202 decrease in freezing during the baseline [no other main effect or interact was detected: (F's < 1.00,
203 p's > 0.30)]. While baseline freezing may impact CS-responding, subtracting baseline responding
204 from CS-elicited freezing (of the first two trials for RANDOM and BW animals) did not eliminate
205 a main effect a drug-treatment ($F_{1,23} = 5.877$, $p < 0.05$). Thus, these data replicate the effects of
206 BNST inactivation on BW CS-elicited freezing as seen in our first experiment and extend these

207 results to show that the BNST mediates freezing to CSs that signal uncertain latency of shock
208 onset.
209
210 ***Temporary inactivation of the BNST does not eliminate fear to a forward CS that is paired with***
211 ***a US of variable intensity.*** To determine whether the BNST is involved in other conditioning
212 procedures imbued with outcome (but not temporal) uncertainty, we examined whether freezing
213 to a FW CS that is paired with a US of variable intensity is also BNST-dependent. In this case, rats
214 received forward fear conditioning with either a fixed ("FIXED") or variable ("VARIABLE") US
215 intensity (Figure 3). A schematic of the behavioral design is shown in Figure 3A; cannula
216 placements are illustrated in Figure 3—Figure Supplement 1. During conditioning (Figure 3B), a
217 repeated measures ANOVA revealed a main effect of trial (repeated measures: $F_{6,168} = 68.15$, $p <$
218 0.0001), with no main effect of drug or conditioning procedure, and no interactions (F's < 1.50,
219 p's > 0.20).
220 Twenty-four hours after conditioning and immediately before a test to the CS in a novel
221 context (Figure 3B), the animals were infused with either muscimol ("MUS") to reversibly
222 inactivate the BNST; saline ("VEH") infusions served as a control. As shown in Figure 3B, BNST
223 inactivation did not eliminate freezing to a FW CS paired with either a fixed or variable US. During
224 retrieval testing, there was a main effect of trial (repeated measures: $F_{6,156} = 24.31$, $p < 0.0001$),
225 however no other main effects or interactions were detected (F's < 2.70, p's > 0.15). Although
226 average baseline freezing was highest in VARIABLE-VEH animals, an ANOVA of baseline
227 freezing did not reveal any main effects or interactions (F's < 3.60, p's > 0.05). To equate for
228 differences in pre-CS freezing in the experimental groups, baseline freezing was subtracted from
229 CS-elicited freezing (Figure 3C). This did not reveal an effect of BNST inactivation on freezing

230 after baseline; there were no significant main effects or interactions in the ANOVA (F's < 0.15,

231 p's > 0.70). In other words, the freezing in the presence of the CS was only increased relative to

232 the baseline and was not masked by it. Although BNST inactivation trended towards reducing

233 generalized contextual freezing in this experiment, it did not eliminate CS-elicited freezing to the

234 temporally predictable cue, regardless of the variable magnitude of the US.

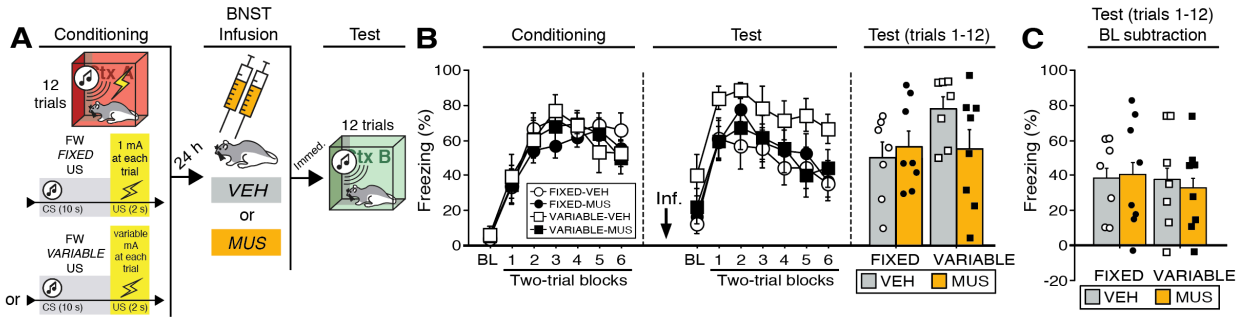

Figure 3. *Temporary inactivation of the BNST does not prevent conditioned fear expression to a forward CS paired with a US of fixed or variable intensity.* **(A)** Behavioral schematic. **(B)** Freezing behavior during conditioning and retrieval testing. For conditioning, the left panel depicts mean percentage freezing during the 5-min baseline (BL) and across each conditioning block (each 138-sec block is comprised of two trials; trials consist of freezing during the 10-sec CS followed by the 58-sec post-shock interval). For retrieval testing, the center panel shows mean percentage freezing at the 5-min baseline (BL) and across each test block (each 140-sec block is comprised of two trials; trials consist of freezing during the 10-sec CS followed by the 60-sec interval). The right panel shows mean percentage freezing across all test trials (after BL; corresponding to 840 sec of behavior). **(C)** Freezing percentages across all twelve trials, with BL levels of freezing subtracted from these values. All data are represented as means ± s.e.m [FIXED-VEH (n = 7); FIXED-MUS (n = 8); VARIABLE-VEH (n = 7); VARIABLE-MUS (n = 8)].

235 ***Backward CSs selectively increase Fos expression in the ventral BNST.*** To further examine the

236 role of the BNST in the expression of conditioned fear, we quantified Fos expression in multiple

237 subregions of the BNST following the presentation of either a FW or BW CS during a shock-free

238 retrieval test (Figure 4). The behavioral design is summarized in Figure 4A. Four experimental

239 groups were compared: rats conditioned and tested to a forward CS ("FW"), rats conditioned and

240 tested to a backward CS ("BW"), rats conditioned to a forward or backward CS but not receiving

241 a CS at test ["NoCS(Test)"], and animals that were conditioned but not tested ("NoTest").
242 Conditioning (Figure 4B) was similar to previous experiments (main effect of trial; repeated
243 measures: $F_{6,258} = 77.346$, $p < 0.0001$; no other main effects or interactions: F's < 1.30, p's > 0.30).
244 As shown in Figure 4B, the groups differed in their levels of conditioned freezing during the
245 retrieval test. ANOVA revealed a main effect of trial (repeated measures: $F_{6,216} = 15.54$, $p <$
246 0.0001), conditioning procedure ($F_{2,36} = 11.42$, $p < 0.0001$), and a procedure × trial interaction
247 ($F_{6,216} = 3.65$, $p < 0.0001$) (includes baseline). Post-hoc analyses revealed that FW ($p < 0.0001$)
248 and BW ($p < 0.005$) rats exhibited significantly higher levels of freezing behavior than NoCS(Test)
249 rats. Similarly, an ANOVA of average freezing across the test trials (without baseline) revealed a
250 main effect of group ($F_{2,36} = 13.76$, $p < 0.0001$). Post-hoc comparisons revealed significant
251 differences between FW vs. BW ($p < 0.05$) and FW vs. NoCS(Test) rats ($p < 0.0001$), as well as
252 BW vs. NoCS(Test) animals ($p < 0.005$).

253 Ninety minutes after the retrieval test, the animals were sacrificed for Fos
254 immunohistochemistry. Fos-positive nuclei were counted in three BNST subregions (Figure 5A):
255 "ovBNST" (Fos counts targeting the oval nucleus of the BNST), "dBNST" (counts in an area
256 containing the dorsal region of the anteromedial BNST), and "vBNST" [Fos counts in a region
257 containing the BNST's anterolateral, fusiform, and anteromedial (ventral) nuclei; refer to
258 (Swanson, 2003)]. As shown in Figure 5B, the average number of Fos-positive nuclei for each of
259 these regions differed in rats undergoing FW or BW conditioning in the ovBNST and vBNST, but
260 not the dBNST. In the vBNST, an ANOVA revealed a main effect of group ($F_{3,43} = 11.41$, $p <$
261 0.0001). Fisher's PLSD revealed that BW rats exhibited significantly higher levels of Fos
262 compared to FW ($p < 0.0005$), NoCS(Test) ($p < 0.001$), and NoTest ($p < 0.0001$) rats. Additionally,
263 NoCS(Test) rats exhibited significantly greater Fos expression than NoTest rats ($p < 0.05$). In the

ovBNST, an ANOVA revealed a main effect of group ($F_{3,43} = 3.26$, $p < 0.05$). Post-hoc analyses revealed that NoTest rats exhibited significantly higher Fos levels compared to FW ($p < 0.05$) and No-CS ($p < 0.01$) rats. In dBNST, there was no effect of conditioning procedure on Fos expression (factorial ANOVA: $F < 2.60$, $p > 0.07$). Together, these data indicate that presentation of a BW CS increases Fos expression in the vBNST. Moreover, exposure to the temporally predictive FW CS (which elicited the highest levels of fear) was associated with low levels of Fos in the BNST.

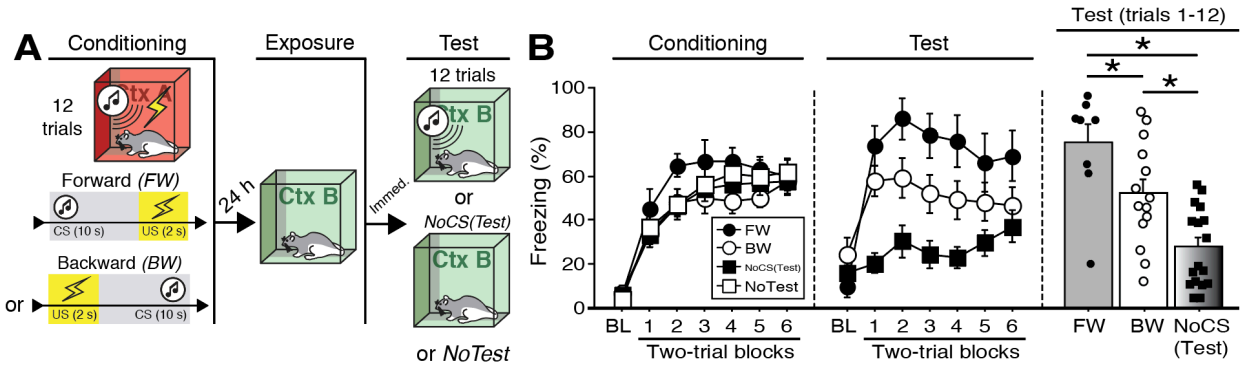

Figure 4. *CS-evoked freezing in rats utilized for Fos analyses.* **(A)** Behavioral schematic. **(B)** Freezing during conditioning and retrieval testing. For conditioning, the left panel depicts mean percentage freezing during the 5-min baseline (BL) and across each conditioning block (each block is comprised of two trials; conditioning trials consist of freezing during the 10-sec CS followed by the 58-sec interstimulus interval). For retrieval testing, the center panel shows mean percentage freezing at the 5-min baseline (BL) and across each test block (each block is comprised of two trials; trials consist of freezing during the 10-sec CS followed by the 60-sec interval). The right panel shows mean percentage freezing after BL. Animals were sacrificed for Fos analyses 90 min after trial 1. All data are represented as means ± s.e.m [FW ($n = 8$); BW ($n = 14$); NoCS(Test) ($n = 17$); NoTest ($n = 8$)]; * = $p < 0.05$.

Backward CSs selectively increase Fos expression in mPFC afferents of the BNST. The BNST receives input from many areas involved in the regulation of fear (Fox and Shackman, 2017; Goode and Maren, 2017; Lebow and Chen, 2016). Therefore, also we used a functional tracing procedure to quantify Fos expression in neurons targeting the BNST (Figure 6). Specifically, rats were injected with a retrograde tracer (CTb-488) into the BNST (prior to conditioning) so that we could quantify Fos expression in BNST-projecting neurons in its major limbic and cortical afferents.

These were the same subjects used for the BNST Fos analyses (see prior section). So, in addition to Fos in the BNST, we quantified fear-elicited Fos in the infralimbic (IL) and prelimbic (PL) regions of the medial prefrontal cortex (mPFC), the basolateral amygdala (BLA), and the ventral hippocampus (HPC). The behavioral data for these animals are shown in Figure 4.

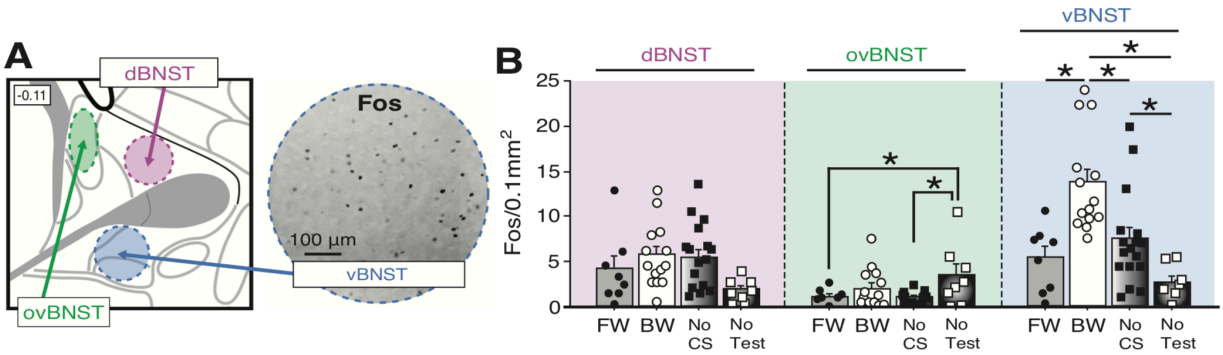

Figure 5. *Fos expression in the BNST following exposure to a temporally predictable or uncertain CS.* **(A)** Schematic depicting regions counted within the BNST (left panel). The right panel shows example of Fos expression in the ventral BNST (vBNST). **(B)** Mean Fos-positive cells per 0.1 mm^2 for each of the quantified regions. All data are represented as means ± s.e.m [FW (n = 8); BW (n = 14); NoCS(Test) (n = 17); NoTest (n = 8)]; * = $p < 0.05$.

A representative image of CTb infusion into the BNST is shown in Figure 6A and an illustration of the largest and smallest CTb spread of injection included in the analyses is shown in Figure 6B. Approximate microinjection sites for CTb for all animals are shown in Figure 6—Figure Supplement 1. Representative Fos and CTb co-labeling is shown in Figure 6C. As shown in Figure 6D, there were reliable differences in CTb labeling among the BNST afferents we quantified. An ANOVA revealed a significant main effect of region ($F_{3,116} = 42.34$, $p < 0.0001$). Post-hoc comparisons indicated that the number of CTb-positive cells in the HPC were significantly higher than that in all other regions ($p < 0.0001$, per comparison); IL and BLA exhibited significantly greater CTb counts compared to PL ($p < 0.0001$, per comparison). CTb counts in each region did not differ by behavioral condition ($F < 0.2$, $p > 0.85$) and were collapsed

290 for Figure 6D. These data indicate extensive connectivity of the PFC, BLA, and HPC with the

291 BNST.

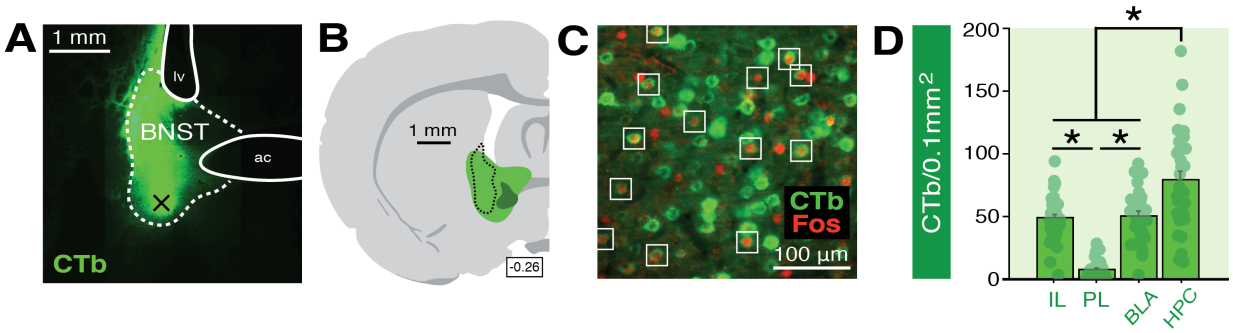

Figure 6. *Functional tracing in afferents targeting the BNST.* **(A)** Coronal section (10×) showing representative fluorescence of a CTb infusion (green) into the BNST (dotted outline; "ac" = anterior commissure, "lv" = lateral ventricle). Black "X" denotes approximate lowest point of the infusion (as an example of how injection sites are documented in Figure 6—Figure Supplement 1). **(B)** Coronal schematic (-0.26 mm from bregma) showing the approximate largest (green) and smallest (dark green) areas of CTb spread in the BNST for animals included in the analyses; the black dotted outline represents the extent of spread of CTb in the BNST in the image shown in panel **A**. **(C)** Example CTb-positive (green) and Fos-positive (red; nuclei) cells in a coronal section (40 µm) of the IL; open white squares denote double-labeled cells. **(D)** Mean number of BNST-targeting CTb-positive cells (per 0.1 mm^2) for each of the quantified regions (shows FW, BW, and NoTest animals corresponding to Figure 8). All data are represented as means ± s.e.m (for each region, $n = 30$); * = $p < 0.05$.

292 As shown in Figure 7A, the number of Fos-positive nuclei in the IL, PL, HPC, and BLA

293 differed among the behavioral groups. Factorial ANOVA of Fos counts in IL revealed a main

294 effect of group ($F_{2,27} = 8.55$, $p < 0.005$). Post-hoc comparisons for IL revealed significant

295 differences between BW vs. NoTest rats ($p < 0.0005$) and FW vs. NoTest rats ($p < 0.05$). In PL, a

296 main effect of group was also identified ($F_{2,27} = 6.79$, $p < 0.005$). Post-hoc analyses indicated that

297 BW rats exhibited significantly more Fos in PL as compared to NoTest animals ($p < 0.001$). For

298 BLA, a main effect of group was detected (factorial ANOVA: $F_{2,27} = 8.10$, $p < 0.005$). Post-hoc

299 analyses revealed that FW and BW rats (which did not significantly differ) exhibited significantly

300 more Fos in BLA as compared to No Test rats ($p < 0.01$, FW vs. NoTest; $p < 0.001$, BW vs.

301 NoTest). In HPC, an ANOVA revealed a significant main effect of group ($F_{2,27} = 4.28$, $p < 0.05$).

302 Post-hoc comparisons indicated that FW and BW rats (again, which did not significantly differ)

303 had significantly more Fos expression in HPC as compared to NoTest animals ($p < 0.05$ for FW
304 vs. NoTest and BW vs. NoTest). These data indicate that conditioned freezing to forward or
305 backward CSs increased the number of Fos-positive neurons in the PFC, BLA, and HPC.

306 To quantify the fraction of BNST-projecting neurons within the PFC, BLA, and HPC that
307 were activated by a FW or BW CS, we calculated a ratio of Fos-positive to CTb-positive nuclei in
308 each afferent region ("Fos-CTb%"; Figure 7B). Interestingly, within the IL, animals in the BW
309 group exhibited the highest fraction of double-labeled cells. An ANOVA revealed a significant
310 main effect of group ($F_{2,27} = 14.22$, $p < 0.0001$). Post-hoc comparisons revealed significant
311 differences between BW and FW rats ($p < 0.005$) as well as BW and NoTest animals ($p < 0.0001$).
312 In contrast, there were no differences between FW and BW rats in any of the other regions
313 quantified. In PL, there was not a significant main effect of group ($F < 1.90$, $p > 0.17$) and no
314 group effects were observed in the BLA ($F < 2.0$, $p > 0.15$). In the HPC, rats in the FW and BW
315 groups exhibited greater numbers of double-labeled cells than those in the NoTest group ($F_{2,27} =$
316 7.82, $p < 0.01$). Additionally, we examined whether freezing significantly correlated with any of
317 the aforementioned Fos measures; gross measures of freezing percentages (trials 1-12) for FW and
318 BW rats did not significantly correlate with Fos levels across the multiple regions (data not shown
319 in figures), suggesting that the presence or absence of the fear CS was more predictive of activity
320 in these circuits than freezing performance *per se*. Nonetheless, these data indicate that conditioned
321 freezing (in both FW and BW rats) is associated with increased activity in BNST-targeting cells
322 of HPC, and that BW CSs selectively increase Fos in BNST-projecting neurons in IL. Hence, IL
323 projections to the BNST may regulate the effects of BW CSs on BNST Fos expression and
324 freezing.

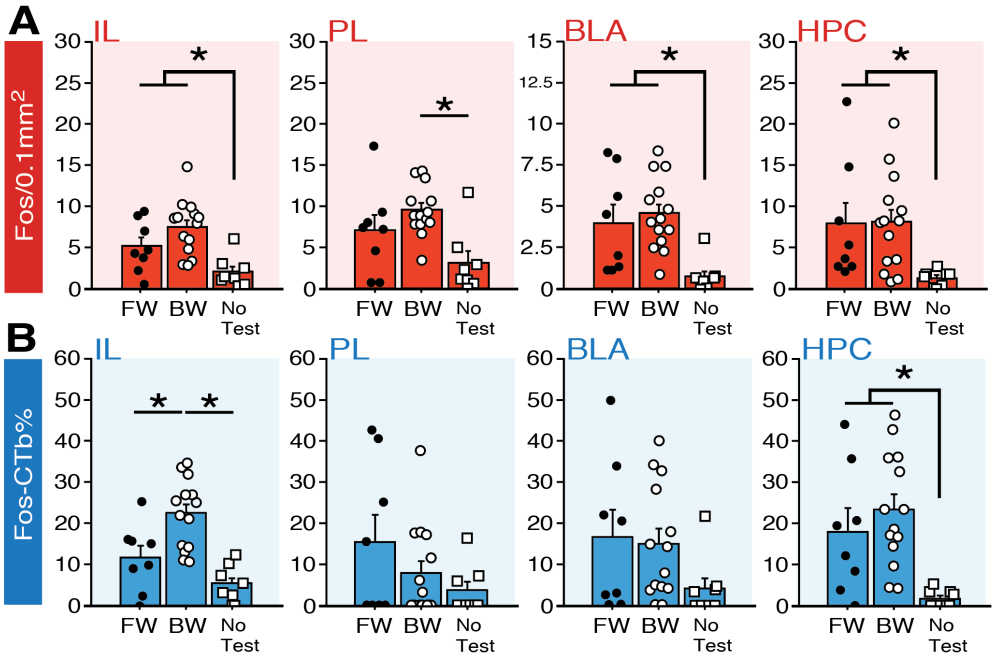

Figure 7. *Fos expression in BNST-targeting cells of the prefrontal cortex, amygdala, and hippocampus following exposure to a forward or backward CS.* **(A)** Mean number of Fos-positive cells (per 0.1 mm^2) for each of the quantified regions. **(B)** Mean percentage (per 0.1 mm^2) of Fos-positive and CTb-positive cells divided by the total number of CTb-positive cells for each region. All data are represented as means ± s.e.m [FW (n = 8); BW (n = 14); NoTest (n = 8)]; * = $p < 0.05$.

DISCUSSION

In the present study, we demonstrate that the BNST is critical for processing unpredictable threats, specifically discrete auditory CSs that are poor predictors of when aversive footshocks will occur. Reversible inactivation of the BNST inactivation disrupted CS-elicited freezing to a backward CS, but did not prevent freezing to a CS that reliably signaled the imminent onset of shock, even when that CS signaled an unpredictable intensity of the US. Moreover, pharmacological blockade of the BNST attenuated fear to both a backward CS and a CS that was trained with random US onset. These data suggest that uncertain timing of shock is a critical factor in recruiting the BNST to conditioned fear. Moreover, BNST inactivation did not affect freezing to a forward CS that was paired with a US that varied in intensity, suggesting that contributions of the BNST to conditioned

336 fear may depend on the type of uncertainty imbued by the CS. Interestingly, freezing to the
337 backward CS was less sustained than that to the forward CS, suggesting that neither long-duration
338 stimuli nor sustained freezing responses are required to recruit the BNST. Finally, although both
339 forward and backward CSs increased Fos expression in the hippocampus, BNST, amygdala, and
340 mPFC, only backward CSs selectively increased Fos expression in both the ventral BNST and
341 BNST-projecting neurons in the infralimbic cortex. Collectively, these data reveal that the BNST
342 and its mPFC afferents may mediate defensive responding to threats that signal uncertain or remote
343 onset of shock.

344 Unpredictable threats come in many forms [including uncertain timing, magnitude or type,
345 or probability of threat: (Bennett et al., 2018; Daldrup et al., 2015; Davies and Craske, 2015;
346 McHugh et al., 2015; McNally et al., 2011; Schroijen et al., 2016; Seidenbecher et al., 2016)];
347 these subtypes of uncertainty may have dissociable and cumulative contributions to anxiety. In
348 particular, uncertainty about the timing of the onset of aversive events has been linked to measures
349 of anxiety in humans and other animals (Amadi et al., 2017; Bennett et al., 2018; Shankman et al.,
350 2011). Interestingly, unpredictable threats (of varying types and degrees) are associated with
351 increases or changes in regional cerebral blood flow and functional connectivity in the primate
352 BNST (Alvarez et al., 2015, 2011; Brinkmann et al., 2018; L Brinkmann et al., 2017; Leonie
353 Brinkmann et al., 2017; Buff et al., 2017; Choi et al., 2014, 2012; Coaster et al., 2011; Fox et al.,
354 2018; Grupe et al., 2013; Herrmann et al., 2016; Kalin et al., 2008, 2005, Klumpers et al., 2017,
355 2015; McMenamin et al., 2014; Meyer et al., 2018; Mobbs et al., 2010; Münsterkötter et al., 2015;
356 Naaz et al., 2019; Pedersen et al., 2018, 2017; Schlund et al., 2013; Sladky et al., 2018; Somerville
357 et al., 2010; Torrisi et al., 2018). In turn, BNST lesions or circuit inactivations reduce defensive
358 responding to contextual cues that poorly signal the imminence of the aversive US [(Asok et al.,

359 2018; Davis and Walker, 2014; Goode et al., 2015; Hammack et al., 2015; Luyten et al., 2011;
360 Poulos et al., 2010; Sullivan et al., 2004; Waddell et al., 2006; Zimmerman and Maren, 2011); but,
361 see (Luyck et al., 2018b)]. Consistent with the possibility that the BNST mediates conditioned fear
362 to temporally uncertain threats, we observed significant and selective decreases in the expression
363 of defensive freezing when we inactivated the BNST in the presence of BW CSs or CSs trained
364 with randomized USs. Conversely, cues that predicted imminent shock were not affected by BNST
365 inactivation. Additionally, we observed significant differences in shock reactivity during forward
366 and backward conditioning, insofar as rats exhibited more robust shock-elicited activity bursts than
367 during forward conditioning. These data may suggest that conditioning in the presence of
368 predictive cues may reduce the magnitude of the unconditioned response, in a way that is not
369 present for the backward CS.

370 A critical finding in the present study is that the BNST mediates conditioned freezing to
371 short-duration discrete CSs. This contrasts with prior work suggesting that the BNST only
372 mediates freezing behavior to long-duration cues or contexts (Hammack et al., 2015; Waddell et
373 al., 2006). However, recent data in other paradigms suggest a role for the BNST in the processing
374 of responses to relatively brief threat stimuli (Brinkmann et al., 2018; Choi et al., 2014; Haufler et
375 al., 2013; Kinnison et al., 2012; Kiyokawa et al., 2015; Klumpers et al., 2017; Luyck et al., 2018b,
376 2018a; Naaz et al., 2019). Together, these data suggest that stimulus duration is not necessarily a
377 determinant of BNST involvement. Similarly, it does not appear that response duration is the
378 primary determinant of the BNST in threat reactions. In the present work, conditioned freezing to
379 the backward CS was generally shorter-lived than that to the forward CS, but was more sensitive
380 to BNST inactivation than freezing to the forward CS. One might conclude from this observation
381 that the BNST mediates weak (but not strong) freezing responses. However, we and others have

382 shown that BNST lesions or inactivation reduce the expression of freezing even when those levels
383 are relatively high (Goode et al., 2015; Hammack et al., 2015). Hence, the BNST mediates fear to
384 cues that signal uncertain or remote threat, independent of the duration of the antecedent stimuli
385 or behavioral responses associated with the threat (Goode and Maren, 2017).

386 Interestingly, it has been suggested that fear to a backward CS relies on associations
387 between the CS and the conditioning context (Chang et al., 2003), which more strongly predicts
388 the US. That is, extinction of fear to the conditioning context reduces fear to a BW, but not FW,
389 CS. Thus, it is possible that the BNST mediates fear expression to a backward CS by retrieving a
390 memory of the context-US association. Indeed, considerable work indicates that BNST is involved
391 in the expression of contextual fear (Davis and Walker, 2014; Goode et al., 2015; Hammack et al.,
392 2015; Luyten et al., 2011; Sullivan et al., 2004; Waddell et al., 2006; Zimmerman and Maren,
393 2011). Increases in immediate early gene expression, metabolic activity, and changes in
394 electrophysiological firing patterns have been observed in the BNST in response to direct exposure
395 to conditioned contextual cues (Campeau et al., 1997; Daldrup et al., 2016; Jennings et al., 2013;
396 Lemos et al., 2010; Luyten et al., 2012; Marcinkiewcz et al., 2016). If the backward CS functions
397 similarly to a conditioned context, then one might expect Fos activity to be elevated in the BNST
398 of animals exposed to the backward CS. Indeed, we observed significantly more Fos expression
399 in the BNST in response to the backward compared to the forward CS. The backward CS-elicited
400 Fos expression was specific to vBNST, insofar as backward and forward rats did not differ in
401 overall levels of Fos in dBNST or ovBNST. Similarly, others have shown elevated Fos expression,
402 in regions in or near vBNST after stress or conditioned fear-related behavior (Besnard et al., 2019;
403 Sterrenburg et al., 2012; Verma et al., 2018; Radley and Johnson, 2018; Radley and Sawchenko,
404 2011).

405 Of course, another possibility is that the backward conditioning procedure yielded forward
406 trace conditioning after the first trial (Burman et al., 2014; Marchand et al., 2004; Raybuck and
407 Lattal, 2014; Tipps et al., 2014). Although there has been considerable work on the neural
408 mechanisms of trace conditioning (Raybuck and Lattal, 2014), a role for the BNST in this form of
409 learning has not yet been established. Because trace conditioning also degrades the temporal
410 imminence of the US following the CS, it might be expected to require the BNST. Consistent with
411 this possibility, we found that inactivation of the BNST reduced fear in the presence of a cue that
412 was conditioned with randomized onset of shock after the CS. In either event, the BNST appears
413 to be recruited by stimuli, whether cues or contexts, that signal remote or temporally unpredictable
414 onset of shock.

415 The amygdala, PFC, and hippocampus have strong connections with the BNST (Canteras
416 and Swanson, 1992; deCampo and Fudge, 2013; Dong et al., 2001; Glangetas et al., 2017; Johnson
417 et al., 2018; McDonald et al., 1999; Reichard et al., 2017; Reynolds and Zahm, 2005; Torrisi et
418 al., 2015; Vertes, 2004; Weller and Smith, 1982; Wood et al., 2018). In line with previous work,
419 the expression of freezing (whether elicited by a forward or, in our case, backward CS) increased
420 the number of Fos-positive neurons in these regions (Herry et al., 2008; Jin and Maren, 2015;
421 Knapska and Maren, 2009; Lemos et al., 2010; Wang et al., 2016). In addition, we found that
422 forward and backward CSs increased Fos expression in BNST-targeting cells of the HPC (with
423 similar, but trending, effects within the BLA). HPC and BLA projections to the BNST are thought
424 to regulate hypothalamic-pituitary-adrenal (HPA) axis activity (Crestani et al., 2013; Forray and
425 Gysling, 2004; Zhu et al., 2001), and these afferents may be engaged in high-fear states to mobilize
426 corticosterone release, for example (Kim et al., 2013). However, unlike the HPC and BLA, we
427 observed a greater number of Fos-positive cells in the IL in response to a backward CS relative to

428 forward CS. This suggests a unique role for BNST-projecting neurons of the IL [which appear to
429 be glutamatergic: (Crowley et al., 2016; Glangetas et al., 2017)] in processing excitatory
430 backwards CSs. There is growing evidence for a regulatory role for prefrontal connections to the
431 BNST in stress and anxiety-like behavior (Fox et al., 2010; Glangetas et al., 2017, 2013; Johnson
432 et al., 2018; Kinnison et al., 2012; Motzkin et al., 2015; Naaz et al., 2019; Radley et al., 2009), the
433 present data adds to this work by suggesting that the IL may be involved in generating freezing
434 and/or stress responding to the backward CS. This would stand in contrast to considerable data
435 indicating that the IL is involved in the inhibition of freezing behavior after extinction, for example
436 (Milad and Quirk, 2002; Quirk and Mueller, 2008). However, the fact that the backward CS elicits
437 less fear (or more extinguishable fear) could suggest this circuit is active, in part, to gate or regulate
438 fear expression. Indeed, there is evidence for a role of the infralimbic cortex in regulating
439 discrimination of conditioned excitors and inhibitors (Sangha et al., 2014). An alternative view is
440 that the IL is involved in processing contextual information conveyed by the hippocampus
441 (Corcoran and Quirk, 2007; Marek et al., 2018; Zelikowsky et al., 2013) during threat processing.
442 To the extent that that backward CSs elicit fear via CS-(context-US) associations (Chang et al.,
443 2003), it is possible that the IL is involved in retrieving CS-context associations.

444 In conclusion, we demonstrate a novel role for the BNST and its circuits in processing
445 discrete cues, including excitatory backward CSs and randomized CSs. Specifically, BNST
446 inactivation impaired conditioned freezing to a backward, but not forward, auditory CS that
447 differed only in their temporal relationship to a footshock US. This reveals that neither stimulus
448 modality nor duration (or response duration) are the critical parameters driving BNST involvement
449 in defensive behavior. We further show that backward CSs increase the number of Fos-positive
450 neurons in the vBNST and in BNST-projecting neurons in the infralimbic cortex. This suggests a

451 novel role for mPFC projections to the BNST in processing unpredictable threats, possibly of the
452 aversive contexts to which backward CSs are associated. These findings may help in our
453 understanding of the broader contributions of the BNST to motivated behaviors that depend on
454 uncertainty, such as during BNST-dependent triggers of fear and drug relapse (Aston-Jones and
455 Harris, 2004; Avery et al., 2016; Goode et al., 2018; Goode and Maren, 2018; Harris and Winder,
456 2018; Miles et al., 2018; Silberman and Winder, 2013; Stamatakis et al., 2014). In total, these
457 experiments provide new insight into the antecedents for BNST-dependent defensive behavior and
458 highlight behavioral procedures to explore these processes.
459
460 **MATERIALS AND METHODS**
461
462 **Subjects.** All experiments used adult (200-240 g upon arrival; n = 285, before exclusions) male
463 Long-Evans rats (Envigo; Indianapolis, IN). Rats were housed in a climate-controlled vivarium
464 and kept on a fixed light/dark cycle (lights on starting at 7:00 AM and off at 9:00 PM; experiments
465 took place during the light phase of the cycle). Rats were individually housed in clear plastic cages
466 (with bedding consisting of wood shavings; changed weekly) on a rotating cage rack. Group
467 assignments for behavioral testing were randomized for cage position on the racks. Animals had
468 access to standard rodent chow and water *ad libitum*. Animals were handled by the experimenter(s)
469 (~30 sec/day) for five consecutive days prior to the start of any surgeries or behavior. All
470 procedures were in accordance with the US National Institutes of Health (NIH) Guide for the Care
471 and Use of Laboratory Animals and were approved by the Texas A&M University Institutional
472 Animal Care and Use Committee.
473

474 **Apparatuses.** All behavioral testing occurred within distinct rooms in the laboratory. Each
475 behavioral room housed eight identical rodent conditioning chambers (30 cm × 24 cm × 21 cm;
476 MED Associates, Inc.). Each chamber was housed in a larger, external sound-attenuating cabinet.
477 Rear walls, ceilings, and the front doors of the testing chambers were made of Plexiglas, while
478 their sidewalls were made of aluminum. Grid floors of the chambers were comprised of nineteen
479 stainless steel bars (4 mm in diameter), and spaced 1.5 cm apart (center to center). The grid floors
480 were attached to an electric shock source and a solid-state grid scrambler for delivery of the US
481 (MED Associates, Inc.). A speaker attached to each chamber was used to deliver the auditory CS.
482 As needed for each context, the chambers were equipped with 15 W house lights, and small fans
483 were embedded in the cabinets (providing background noise of ~70 dB). An aluminum pan was
484 inserted beneath the grid floor to collect animal waste. A small camera was attached to the top of
485 the cabinet for video monitoring of behavior.

486 Measurements of freezing were performed using an automated and unbiased system
487 (Maren, 1998). Specifically, each behavioral testing chamber rested on a load-cell platform that
488 was sensitive to cage displacement due to the animal's movements. During behavioral testing,
489 load-cell activity values (ranging from -10 to +10 V) were collected and digitized at 5 Hz using
490 Threshold Activity Software (MED Associates, Inc.). Offline conversions of the load-cell activity
491 values were performed to generate absolute values ranging from 0 to 100; lower values indicate
492 minimal cage displacement, which coincided with freezing behaviors in the chambers.
493 Accordingly, freezing bouts were defined as absolute values of ≤10 for 1 s or more. The percentage
494 of freezing behavior during the pre-CS baseline, the CS, and the inter-trial intervals was computed
495 for each behavioral session. Shock reactivity was analyzed by directly reporting the absolute

496 values generated by the Threshold Activity Software (i.e., larger values indicated more movement
497 in the cage).
498 Unique contexts (A and B) were used for conditioning retrieval testing. Chamber
499 assignments were unique to each context and group assignments were counterbalanced across test
500 chambers when possible. For each experiment, context A was assigned to one of the behavioral
501 rooms, and B the other. For context A, the test chamber was wiped down with an acetic acid
502 solution (3%) and a small amount was poured in the pans beneath the grid floors. The cage lights
503 were turned on, while the chamber fans were turned off. The cabinet doors were closed. The
504 behavioral room was illuminated with dim red light. Animals were transported to and from the
505 chambers using white plastic transport boxes. For context B, an ammonium hydroxide solution
506 (1%) was used to wipe down and scent the chambers, black Plexiglas panels were placed over the
507 grid floors, the cage lights were turned off, the chamber fans were turned on, and the cabinet doors
508 remained open. The behavioral room was illuminated with white light (red room lights were turned
509 off). Rats were transported to and from the context using black plastic transport boxes that included
510 a layer of clean bedding.
511
512 **Surgeries.** For animals receiving intracranial microinfusions into the BNST, rats were transported
513 to the surgical suite and deeply anesthetized using isoflurane (5% for induction, 1-2% for
514 maintenance) (Acca et al., 2017; Goode et al., 2015; Nagaya et al., 2015; Zimmerman and Maren,
515 2011). Rats were then secured in a stereotaxic frame (Kopf Instruments). Hair on top of the
516 rodent's head was shaved, povidone-iodine was applied, and a small incision was made in the scalp
517 to expose the skull. Bregma and lambda were aligned on a horizontal plane, and small holes were
518 drilled in the skull for the placement of anchoring screws and bilateral stainless-steel guide

519 cannulas (26 gauge, 8 mm from the bottom of their plastic pedestals; Small Parts). The cannulas
520 were inserted into the BNST at the following coordinates: -0.15 mm posterior to bregma, ±2.65
521 mm lateral to the midline, and -5.85 mm dorsal to dura (guide cannulas were angled at 10° with
522 their needles directed at the midline). Dental cement was used to secure the cannulas to the screws
523 and stainless steel obturators (33 gauge, 9 mm; Small Parts) were inserted into the guide cannulas.
524 Animals were given at least one week to recover prior to the onset of behavioral training.
525 For rats injected with cholera toxin subunit B (CTb) conjugated with Alexa Fluor-488
526 (CTb-488; ThermoFisher Scientific) in the BNST, the surgical procedures were identical to those
527 described above. A single small hole was drilled into the skull to allow for the insertion of a glass
528 micropipette. Injection tips were backfilled with mineral oil and secured in the injector; CTb-488
529 was then drawn up into the injector immediately before use. Rats received unilateral CTb-488
530 infusions into either the left or right hemisphere (group assignments were randomized for sites of
531 CTb-488 infusion): -0.15 mm posterior to bregma, ±2.65 mm lateral to the midline, and -6.50 mm
532 dorsal to dura (the pipette was angled at 10° with the tip directed at the midline). CTb-488 (5.0
533 mg/µl; total volume of 0.25 µl) was microinfused into the brain using a Nanoject II auto-nanoliter
534 injector (Drummond Scientific Co.) secured to the arms of the stereotaxic frame. For the infusion
535 process, 50 nl (25 nl/s) of CTb-488 was infused once per min for 5 min to achieve 0.25 µl of the
536 total infusion (the injection needle was left in the brain for 5 additional minutes to allow for
537 diffusion of CTb-488). Following the infusion procedures, the incision was closed with sutures
538 and the animals were returned to their homecages where they recovered for ~10 days.
539
540 **Intracranial infusions.** Prior to behavioral testing, the animals were acclimated to the process of
541 intracranial infusions. On two occasions, the animals were transported from the vivarium to the

542 infusion room in 5-gallon buckets containing a layer of bedding; the experimenter(s) removed the
543 obturators and replaced them with clean ones. On the day of infusions, animals (in predetermined
544 squads of four to eight rats; representing all drug/behavioral groups as possible) were transported
545 to the laboratory, obturators were removed, and injectors were inserted into the guides. Stainless
546 steel injectors (33 gauge, Small Parts; 9-mm extending 1 mm beyond the end of the guide cannula)
547 were connected to polyethylene tubing (PE-20; Braintree Scientific); the other end of the tubing
548 was connected to gastight 10 μl syringes (Hamilton, Co.). The syringes were mounted to an
549 infusion pump (KD Scientific, Inc.). For the experiments shown in Figure 1 and Figure 1—Figure
550 Supplement 3, the α-amino-3-hydroxy-5-methyl-4-isoxazolepropionic acid (AMPA) receptor
551 antagonist 2,3-dihydroxy-6-nitro-7-sulfamoyl-benzo[f]quinoxaline-2,3-dione (NBQX) was used
552 to reversibly inactivate the BNST (Adami et al., 2017; Davis and Walker, 2014; Goode et al., 2015;
553 Zimmerman and Maren, 2011). NBQX disodium salt hydrate (Sigma Life Sciences) was dissolved
554 in saline to a concentration of 10.0 μg/μl ("NBQX"); physiological saline served as the vehicle
555 ("VEH" for all experiments). For the experiments shown in Figure 2 and 3, the γ-aminobutyric
556 acid $(GABA)_A$ receptor agonist muscimol was used to reversibly inactivate the BNST (Bangasser
557 et al., 2005; Breitfeld et al., 2015; Buffalari and See, 2011; Fendt et al., 2003; Goode et al., 2015;
558 Markham et al., 2009; Pina et al., 2015; Sajdyk et al., 2008; Xu et al., 2012). Muscimol (Sigma-
559 Aldrich) was dissolved in physiological saline to a concentration of 0.1 μg/μl ("MUS" for Figure
560 3 and 5); physiological saline served as the vehicle ("VEH"). Although both drugs have been used
561 to inactivate the BNST (see above), we used NBQX and muscimol in separate experiments to
562 observe whether one was more effective in attenuating FW- or BW-elicited behavior; both drugs
563 appeared effective in reducing BW CS-elicited freezing. For the representative image showing
564 drug spread in the BNST (Figure 1—Figure Supplement 1), muscimol TMR-X conjugate (Thermo

565 Fisher Scientific) was dissolved in physiological saline to a concentration of 0.1 μg/μl and used
566 for infusions. For all of the aforementioned experiments, drug or vehicle was drawn into the
567 injectors (immediately prior to the infusions) and a total volume of 0.275 μl/hemisphere of drug
568 or vehicle was infused at a rate of 0.275 μl/min; injectors were left in the cannulas for 1 min
569 following the infusions to allow for diffusion. Once the injectors were removed, clean obturators
570 were inserted into the guides.
571
572 **Behavioral procedures and exclusions.** Overviews of each behavioral experiment are provided
573 in the figures. The conditioned stimulus (CS) for all experiments was an auditory tone (80 dB, 2
574 kHz, 10 sec), which was paired with the unconditioned stimulus (US, footshock; 1.0 mA, 2 sec).
575 For the variable shock intensity experiment (Figure 4), US intensity varied as described.
576 *FW/BW/NoCS(Test) BNST inactivation (twelve training trials).* In a 3 × 2 design, animals
577 (n = 64, prior to exclusions) were randomly assigned to receive a CS at test [either a forward
578 ("FW")- or backward ("BW")-trained CS] or no CS at test [animals were trained to a BW CS;
579 "No-CS"], and NBQX ("NBQX") or vehicle infusions ("VEH"). Of these rats, seven were
580 excluded due to off-target cannulas, three additional rats were excluded due to illness, and four
581 more were excluded due to a technical error during infusions that resulted in no drug or vehicle to
582 be infused (fourteen total exclusions). This resulted in the following (final) group numbers (shown
583 in data/figures): FW-VEH (n = 5); FW-NBQX (n = 4); BW-VEH (n = 13); BW-NBQX (n = 12);
584 No-CS-VEH (n = 8); No-CS-NBQX (n = 8). For conditioning, animals (in squads of eight rats)
585 were transported from the vivarium to context A; FW and BW procedures were run in alternating
586 squads of animals. Drug and vehicle assignments were counterbalanced for position in the
587 chambers. For FW conditioning, were placed in the context for 5 min before the delivery of twelve

588 CS-US trials (CS offset immediately preceded US onset; 70-sec intertrial interval). After the final
589 conditioning trial, the animals remained in the chamber for 1 min before being returned to their
590 homecages (the entire conditioning session consisted of 19 min total; for both FW and BW
591 conditioning). For BW conditioning, all aspects of conditioning were identical to the FW training
592 except the order of the CS and US was reversed. That is, after a 5-min baseline period, the animals
593 received 12 US-CS trials (the onset of the CS occurred immediately after the offset of the US; 70-
594 sec intertrial intervals). After conditioning, rats were returned to their homecages.

595 Twenty-four hours after conditioning, animals (in squads of four) were infused with NBQX
596 or VEH into the BNST immediately before being placed in context B. After 5 min of acclimation
597 to the context, FW and BW animals (intermixed in each squad) received twelve presentations of
598 the CS in the absence of the US (70-sec intertrial interval). The rats remained in the chambers for
599 1 min following the final CS (19 min session, in total). For rats not receiving the CS at test, the
600 animals remained in the test context for 19 min without presentation of the CS or US. We alternated
601 running squads that received the CS and those that did not after the infusions. Following the test,
602 animals were returned to their homecages.

603 *FW/BW BNST inactivation (five training trials).* In a 2 × 2 design, animals (n = 28, prior
604 to exclusions) were randomly assigned to receive forward ("FW") or backward ("BW")
605 conditioning using five training trials, and NBQX ("NBQX") or vehicle infusions ("VEH"). Of
606 these rats, three were excluded due to off-target cannulas. This resulted in the following (final)
607 group numbers (shown in data/figures): FW-NBQX (n = 6); FW-VEH (n = 6); BW-NBQX (n =
608 6); BW-VEH (n = 7). At the start of behavior, rats (in squads of seven) were transported from the
609 vivarium and placed in context A. We alternated squads that received forward or backward
610 conditioning. For forward conditioning, rats were given 3 min of acclimation to the context prior

611 to the onset of five CS-US trials. Rats remained in the chamber for 1 min following the final trial
612 (530 sec total conditioning session). For backward conditioning, rats were placed in context a for
613 a 3-min baseline (530 sec session total), after which they received five US-CS trials. Rats were
614 returned to their homecages after conditioning. Twenty-four hours after conditioning, the animals
615 were placed in context B in the absence of the CS or US for 530 sec to acclimate them to the test
616 context. After this acclimation session, rats were again returned to their homecages.

617 Forty-eight hours after conditioning, the animals received NBQX or VEH infusions
618 (identical to above) immediately prior to retrieval testing. FW and BW animals were intermixed
619 in each squad. Immediately after the infusions, animals were placed in context B for a retrieval
620 test to assess freezing to the CS. The test (530 sec in total) consisted of a 3-min baseline period
621 followed by five CS-alone presentations (70-s intertrial interval). Rats were returned to their
622 homecages following the test session.

623 *FW/BW intra-shock reactivity.* Rats (n = 32, no exclusions) were randomly assigned to
624 receive forward ("FW") or backward ("BW") conditioning. No rats were excluded from this
625 experiment (no infusions occurred; n = 16, per group); only data from the conditioning session are
626 shown. Animals (in squads of eight) were transported to context A for either FW or BW
627 conditioning. Parameters for FW and BW conditioning were identical to the procedures for the
628 previous 12-trial experiments. We alternated FW and BW squads. Rats were returned to their
629 homecages following training.

630 *RANDOM/BW/NoCS(Cond) BNST inactivation.* In a 3 × 2 design, rats (n = 70, prior to
631 exclusions) were randomly assigned to receive backward conditioning ("BW"; identical to the 12-
632 trial BW conditioning described above), randomized CS/US trials in which the duration of the
633 intervals between CS offset and US onset vary on each trial ("RANDOM"), or US-only contextual

634 conditioning [shock intervals matched the RANDOM group; "NoCS(Cond)"]. Of these groups,
635 animals were randomly assigned to receive muscimol ("MUS") or vehicle ("VEH") infusions
636 immediately prior to retrieval. For this experiment, 30 animals were excluded due to off-target
637 cannulas. This resulted in the following (final) group numbers (shown in data/figures): BW-VEH
638 (n = 5); BW-MUS (n = 7); RANDOM-VEH (n = 6); RANDOM-MUS (n = 9); NoCS(Cond)-VEH
639 (n = 7); NoCS(Cond)-MUS (n = 6).

640 For conditioning, animals (in squads of five to eight rats; counterbalanced for the type of
641 conditioning) were transported to context A and underwent BW, RANDOM, or NoCS(Cond)
642 training. Drug and vehicle assignments were counterbalanced for the conditioning procedure and
643 chamber placements for each squad. For BW animals, the conditioning parameters matched those
644 used for the 12-trial experiment described above. For RANDOM animals, and after the 5-min
645 baseline, CS presentations matched the 60 s interstimulus intervals used for the 12-trial FW
646 paradigms (noted above); US onset occurred at the following intervals after offset of each CS at
647 each trial: 26 s, 52 s, 10 s, 40 s, 16 s, 52 s, 14 s, 50 s, 18 s, 36 s, 48 s, 6 s (the entire session last 19
648 min). For NoCS(Cond) animals, rats experienced the same protocol as the RANDOM group, but
649 no auditory CS occurred. Rats were returned to their homecages following conditioning.

650 Twenty-four hours later, animals (in squads of four to six) were transported to the
651 laboratory to receive pre-retrieval infusions of MUS or VEH (counterbalanced in each squad).
652 BW, RANDOM, and NoCS(Cond) animals were intermixed in each squad. Immediately after the
653 intracranial infusions, and after a 5-min baseline in context B, each squad of rats received twelve
654 presentations of the CS in the absence of the US. Each CS presentation was separated by 70 sec
655 intertrial intervals, with the entire test lasting 19 min. Rats were returned to their homecages
656 following the test session.

657 *FIXED/VARIABLE BNST inactivation.* In a 2 × 2 design, rats (*n* = 31, prior to exclusions)
658 were randomly assigned to receive forward conditioning with consistent ("FIXED") or variable
659 magnitudes of the US ("VARIABLE"); muscimol ("MUS") or vehicle ("VEH") infusions were
660 made prior to retrieval testing. For FIXED animals, US intensity was 1 mA at each trial. For
661 VARIABLE animals, shock intensity (in mA) varied across trials in this order (mean = 1 mA):
662 0.5, 1.8, 0.4, 1.6, 1.4, 0.3, 0.5, 1.8, 0.4, 1.6, 1.4, 0.3. In this experiment, one rat was excluded due
663 to off-target cannulas. This resulted in the following (final) group numbers (shown in data/figures):
664 FIXED-VEH (*n* = 7); FIXED-MUS (*n* = 8); VARIABLE-VEH (*n* = 7); VARIABLE-MUS (*n* =
665 8).

666 For conditioning, animals (in squads of seven to eight) were transported to context A
667 (squads alternated between FIXED and VARIABLE paradigms). The rats were given 5 min to
668 acclimate to the context before the onset of 12 CS-US pairings (70-sec intertrial intervals). Rats
669 remained in the chambers for 1 min following the final CS, with the entire conditioning session
670 lasting 19 min. Rats were returned to their homecages following conditioning.

671 Twenty-four hours later, rats (in squads of seven to eight) received intracranial infusions
672 of MUS or VEH into the BNST immediately before being placed in context B for retrieval testing.
673 Rats were given a 5-min baseline period before the onset of twelve CS-alone presentations (70-
674 sec intertrial intervals). Rats remained in the chambers for 1 min following the final CS, with the
675 entire test session lasting 19 min. Rats were returned to their homecages following the test.

676 *FW/BW Fos-CTb.* Animals (*n* = 60, before exclusions) were randomly assigned to receive
677 a forward ("FW")- or backward ("BW")-trained CS at testing, or no CS retrieval at test
678 ["NoCS(Test)"]. Note that the No-CS group consists of animals that were trained to either a FW
679 or BW CS. Additionally, a group of BW-trained animals remained in their homecages ("NoTest")

680 during the final test and were sacrificed alongside the other groups. Twelve rats were excluded for
681 either excessive or off-target infusion of CTb-488 outside the borders of the BNST or an absence
682 of CTb-488 labeling in the ventral BNST. One additional rat was excluded due to a technical issue
683 that resulted in the loss of tissue at the level of the prefrontal cortex. This resulted in the following
684 (final) group numbers (shown in data/figures): FW (n = 8); BW (n = 14); NoCS(Test) [n = 17
685 (BW-trained: n = 9; FW-trained: n = 8)]; NoTest (n = 8). For behavioral training, rats (in squads
686 of six to eight; with all groups intermixed) were transported to the laboratory and placed in context
687 B to acclimate for 5 min (no CS or US) and then returned to their homecages. Later that day, the
688 animals were transported to context A where they received twelve trials of either FW or BW fear
689 conditioning, which was identical to the other aforementioned procedures. We alternated FW and
690 BW conditioning squads. After conditioning, the rats were returned to their homecages. Twenty-
691 four hours after conditioning, all rats were exposed to context B for 20 min in the absence of the
692 CS or US to acclimate them to the test context.

693 Forty-eight hours later, FW, BW, and NoCS(Test) rats were transported to context B to
694 receive a retrieval test to the CS or were merely placed in the context [NoCS(Test) condition].
695 Squads alternated between the CS and no CS test. For rats undergoing CS retrieval, FW and BW
696 animals (intermixed in each squad) received CS trials as described previously. Rats were perfused
697 90 min following the first CS of the test, in groups of three to four. For NoCS(Test) rats (with FW-
698 and BW-trained animals intermixed), animals were exposed to context B in the absence of the CS
699 or US. NoCS(Test) rats were perfused 95 min after being placed in the test context, in groups of
700 three to four. NoTest rats were perfused alongside groups of FW, BW, and No-CS rats. Rats were
701 returned to their homecages after testing and prior to the perfusions.
702

703 **Histological procedures.** At the conclusion of behavioral testing, cannula-implanted animals were
704 overdosed with sodium pentobarbital (Fatal Plus; 100 mg/ml, 0.5 ml, i.p.). Transcardial perfusions
705 were then performed using chilled physiological saline followed by 10% formalin. Brains were
706 extracted and stored in 10% formalin for 24 hr at 4° C; brains were transferred to a 30% sucrose-
707 formalin solution for three or more days (at 4° C) before sectioning. Brains were flash frozen with
708 crushed dry ice and coronal sections (40 μm) containing the BNST were collected using a cryostat
709 (Leica Microsystems) at -20° C. The tissue was wet-mounted to gelatin-subbed microscope slides
710 and stained with 0.25% thionin prior to adding glass coverslips secured with mounting medium
711 (Permount, Sigma). To further examine the spread of drug, a subset of animals was infused
712 (identical to the aforementioned infusion parameters) with fluorescent muscimol (1.0 μg/μl;
713 EverFluor TMR-X conjugate, Setareh Biotech) before being sacrificed (these animals were not
714 perfused) and having brains dissected (40 μm; brains were stored in 30% sucrose solution at 4° C
715 until sectioning). These tissues were wet-mounted to slides and aqueous mounting medium
716 (Fluoromount; Sigma-Aldrich) was used to secure glass coverslips.
717 For CTb-injected animals, post-behavior perfusions mirrored the aforementioned
718 procedures. For sectioning, coronal sections (which included regions of the prefrontal cortex,
719 BNST, basolateral amygdala, and ventral hippocampus) were collected into well plates containing
720 phosphate-buffered saline (1× PBS) and stored in the dark at 4° C until immunohistochemistry
721 could be performed. For localization of the CTb-injection site, separate sections at the level of the
722 BNST were wet-mounted and coverslipped using Fluoromount mounting medium.
723
724 **Immunohistochemistry.** Immunohistochemistry for Fos was performed on free-floating brain
725 tissue similar to prior reports (Jin and Maren, 2015; Marek et al., 2018; Orsini et al., 2011; Wang

726 et al., 2016). For sections containing the BNST, Fos was stained using the following procedures
727 [all steps were performed at room temperature (~20° C) on a shaker, unless stated otherwise; rinses
728 were brief (~20 sec)]. The tissue was first rinsed in 1× tris-buffered saline (TBS; 7.4 pH), and then
729 incubated in 0.3% H_2O_2 (in TBS) for 15 min, followed by rinses (×3) in TBS. Slices were
730 transferred to primary antibody [rabbit anti-c-fos, 1:10,000 in 1× TBS containing Tween 20
731 (TBST); Millipore] and incubated overnight. Sections were then rinsed (×3) in TBS before
732 incubating in secondary antibody for 1 hr (biotinylated goat anti-rabbit, 1:1,000 in TBST; Jackson
733 Immunoresearch). Sections were rinsed (×3) again in TBS. The slices were transferred to wells
734 containing avidin biotin complex (ABC, 1:1,000 in TBST; Vector Labs) for 45 min. The tissues
735 were again rinsed (×3) in TBS. Tissue was transferred to wells containing 3,3′ diaminobenzidine
736 [(DAB) 5% stock, 1:200], nickel ammonium sulfate (5% stock, 1:10), and 30% H_2O_2 (1:2,000) in
737 TBS for 10 min to generate purple/black nuclear chromophore products. After another rinse (×3)
738 in TBS, the tissue was subsequently wet-mounted to slides and secured with coverslips using
739 Permount mounting medium.

740 For sections containing the prefrontal cortex, amygdala, and hippocampus (Fos-CTb
741 experiment), Fos was stained using the following procedures [unless stated otherwise, each step
742 occurred at room temperature (~20° C) on a shaker (and away from excess light)]. First, the tissue
743 was rinsed (10 min; ×2) in 1× TBS, followed by a 10 min wash in 1× TBST. The tissue was
744 incubated in 10% normal donkey serum (NDS; in TBST) for 1 hr. The slices were then rinsed (5
745 min; ×2) in TBST. Sections were transferred to primary antibody [goat anti-c-fos, 1:2,000 in 3%
746 NDS (in TBST); Santa Cruz Biotechnology] and incubated on a rotator in the dark for 72 hr at 4°
747 C. The tissue was rinsed (10 min; ×3) in TBST before incubating in secondary antibody
748 [biotinylated donkey anti-goat, 1:200 in 3% NDS (in TBST); Santa Cruz Biotechnology] for 2 hr.

749 Slices were then rinsed (10 min; ×3) in TBST. Sections were transferred to wells containing
750 streptavidin (Alexa-Fluor 594-conjugate, 1:500 in 3% NDS (in TBST); Thermo Fisher Scientific]
751 for 1 hr. Tissue was rinsed (10 min; ×3) in TBS before being wet-mounted to slides and secured
752 with coverslips using Fluoromount mounting medium.
753
754 **Image analyses.** All imaging and counting procedures (for all regions) were performed with the
755 experimenter(s) blind to the group assignments of the animals. For thionin-stained coronal tissue,
756 photomicrographs of cannula in the BNST were generated (10× magnification) using a Leica
757 microscope (MZFLIII) and Leica Firecam software. For animals infused with fluorescent
758 muscimol into the BNST, infusion sites were imaged (10× magnification) using a Zeiss
759 microscope and Axio Imager 2 software (Zen Pro 2012). For CTb-injected animals, BNST images
760 were generated (10× magnification) using the same Zeiss microscope and software.
761 For Fos analyses in BNST, brightfield images of BNST [in BNST regions ranging from
762 approximately -0.00 to -0.50 mm posterior to bregma of the skull, and from both left and right
763 hemispheres (randomized for site of CTb-injection)] were generated (10× magnification) using a
764 Zeiss microscope and Axio Imager 2 software (Zen Pro 2012). ImageJ software (Schneider et al.,
765 2012) was used to count cells. Counts were confined to the following areas of interest: (1)
766 "ovBNST" [an area of 0.217 mm × 0.558 mm (oval); targeting the oval nucleus of the BNST], (2)
767 "dBNST" [0.372 mm^2 (circle); targeting the dorsal and medial subregions of the anterior BNST,
768 including the anteromedial area of the BNST (dorsal to the anterior commissure)], and (3)
769 "vBNST" [0.434 mm^2 (circle); targeting the ventral regions (ventral to the anterior commissure)
770 of the anterior BNST, which includes the ventral portion of the anteromedial area, the anterolateral
771 area, and the fusiform nucleus of the BNST] (Swanson, 2003). For each of these regions, three to

772 six images were quantified and averaged for each animal (Fos levels were standardized to 0.1
773 mm^2).

774 For Fos-CTb analyses in the prefrontal cortex, amygdala, and hippocampus, images (10×
775 magnification) of Fos and CTb expression were generated using a Zeiss microscope and Axio
776 Imager 2 software (Zen Pro 2012). Cell counts were analyzed using ImageJ software. Images were
777 generated and analyzed only for the hemisphere injected with CTb. Counts were confined to the
778 following areas of interest: (1) "IL" [an area of 0.805 mm × 0.217 mm (rectangle); targeting deep
779 and superficial layers of the infralimbic cortex (approximately +2.0 to +3.2 mm anterior to bregma
780 of the skull)], (2) "PL" [1.115 mm × 0.217 mm (rectangle); targeting deep and superficial layers
781 of the prelimbic cortex (approximately +2.0 to +3.2 mm anterior to bregma of the skull)], (3)
782 "BLA" [0.434 mm^2 (circle); targeting the basolateral amygdala (approximately -1.8 to -3.5 mm
783 posterior to bregma of the skull)], and (4) "HPC" [0.496 mm × 0.217 mm (rectangle); targeting
784 the ventral subiculum but may include some CA1 cells of the ventral hippocampus (approximately
785 within -4.7 to -7.0 mm posterior to bregma of the skull)] (Swanson, 2003). For each of these
786 regions, three to six images were quantified and averaged for each animal (all counts and
787 percentages were normalized to 0.1 mm^2).

788

789 **Statistics.** All data were submitted to repeated or factorial analysis of variance (ANOVA) or two-
790 tailed *t*-tests as described for each experiment. Fisher's protected least significant difference
791 (PLSD) test was used for *post hoc* comparisons of group means following a significant omnibus *F*
792 ratio in the ANOVA (α was set at 0.05). No statistical methods were used to predetermine group
793 sizes (group sizes were selected based on prior work and what is common for the field). Data

794 distributions were assumed to be normal, but these were not formally tested. Unless stated
795 otherwise, all data are represented as means ± s.e.m.
796
797 **ACKNOWLEDGEMENTS**
798 The authors thank Carolyn Evemy, Kaitlyn French, and Sohmee Kim for technical assistance.
799 Supported by grants from the National Institutes of Health (R01MH065961 and R01MH117852
800 to S.M. and F31MH107113 to T.D.G.), as well as a McKnight Foundation Memory and Cognitive
801 Disorders Award and a Brain & Behavior Research Foundation NARSAD Distinguished
802 Investigator Grant to S.M.
803
804 **ADDITIONAL INFORMATION**
805 **Competing interests**
806 The authors declare no competing interests.
807
808

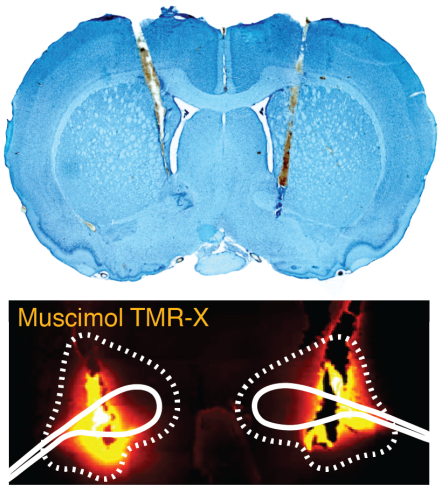

Figure 1—Figure Supplement 1

Representative bilateral cannula placements in the BNST. Photomicrograph (10×) of a thionin-stained coronal section depicting representative cannula tracts in the BNST (top panel). Fluorescent image (gold filter) of a coronal section (10×) showing spread of drug in BNST (BNST outlined in dotted line) (bottom panel).

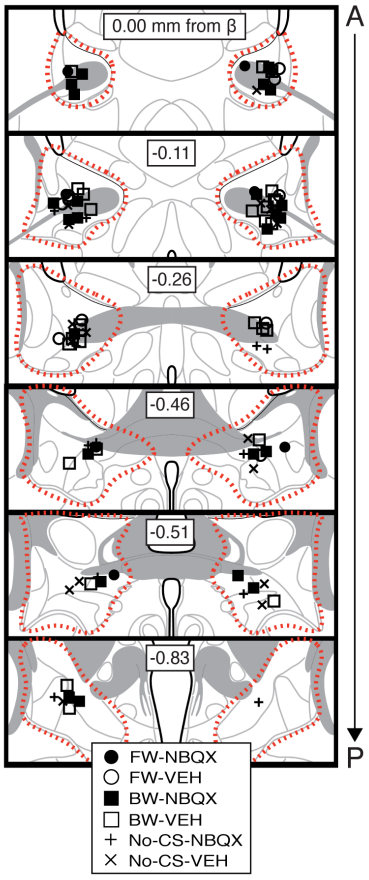

Figure 1—Figure Supplement 2
Bilateral cannula placements for BNST microinfusions. Schematic depicting cannula placements for Figure 1. Symbols (split by each group) correspond to injector tips (approximate borders of BNST are shown by red dotted outline; approximate borders of BNST are shown by red dotted outline).

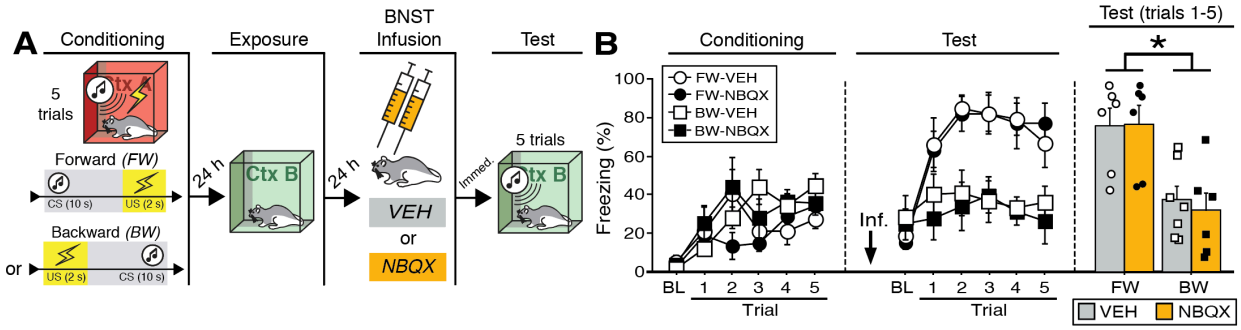

Figure 1—Figure Supplement 3

Effects of BNST inactivation on freezing to a forward vs. backward CS trained with five trials. **(A)** Behavioral schematic. **(B)** Freezing behavior during conditioning and retrieval testing. For conditioning, the left panel depicts mean percentage freezing during the 3-min baseline (BL) and across each conditioning block (each 138-sec block is comprised of two trials; conditioning trials consist of freezing during the 10-sec CS followed by the 58-sec interstimulus interval). For retrieval testing, the center panel shows mean percentage freezing at the 3-min baseline (BL) and across each test trial (each trial consists of freezing during the 10-sec CS followed by the 60-sec interstimulus interval). The right panel shows mean percentage freezing after baseline (trials 1-5; corresponding to 350 sec of behavior). All data are represented as means ± s.e.m [FW-VEH (n = 6); FW-NBQX (n = 6); BW-VEH (n = 7); BW-NBQX (n = 6)]; * = $p < 0.05$.

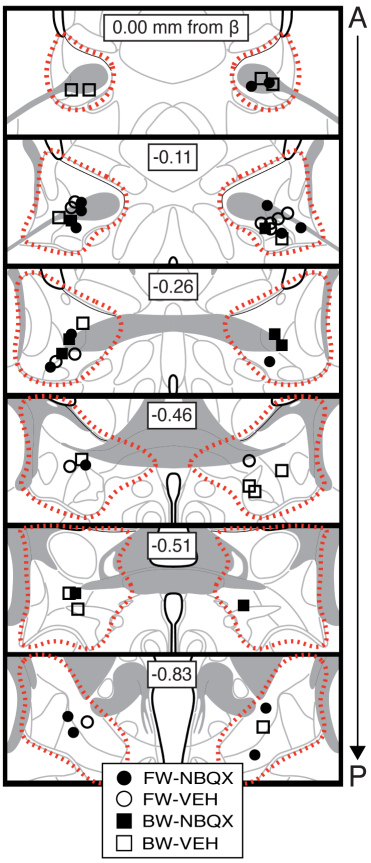

Figure 1—Figure Supplement 4
Bilateral cannula placements for BNST microinfusions. Schematic depicting cannula placements for Figure 1—Figure Supplement 3. Symbols (split by each group) correspond to injector tips (approximate borders of BNST are shown by red dotted outline).

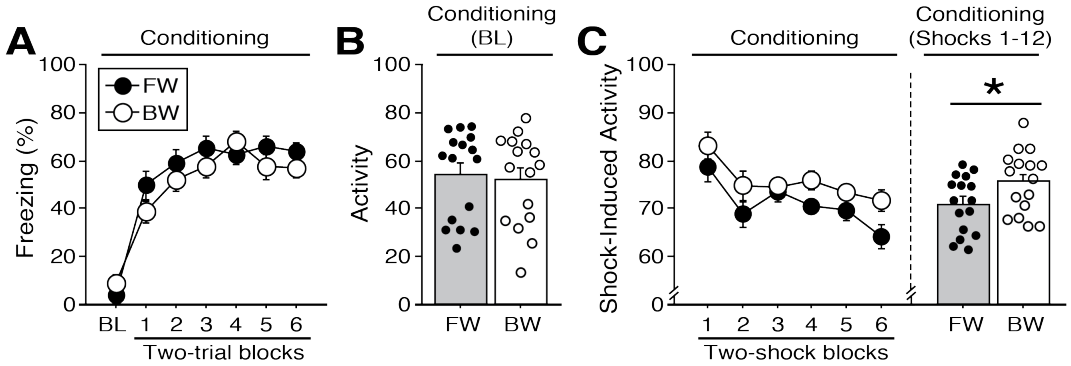

Figure 1—Figure Supplement 5. *Shock-induced activity during conditioning to a forward vs. backward CS.* **(A)** Mean percentage of freezing at baseline (BL; 5-min) and across conditioning blocks (each 138-sec block is comprised of two trials; trials consist of freezing during the 10-sec CS followed by the 58-sec interstimulus interval). **(B)** Mean activity values across the 5-min BL (no shock present). **(C)** The left panel shows mean shock-induced activity (during shocks) at conditioning [averaged into 4-sec (two-shock) blocks]. The right panel shows mean shock-induced activity across all trials. All data are represented as means ± s.e.m [FW (n = 16); BW (n = 16)]; * = $p < 0.05$.

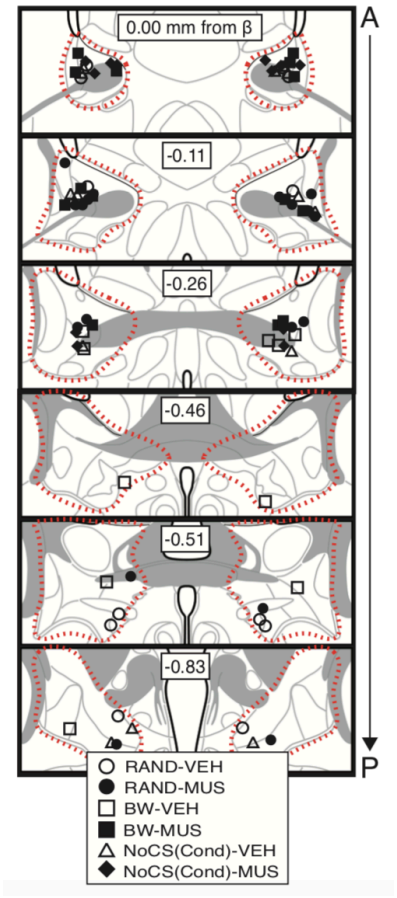

Figure 2—Figure Supplement 1
Bilateral cannula placements for BNST microinfusions. Schematic depicting cannula placements for Figure 2. Symbols (split by each group) correspond to injector tips (approximate borders of BNST are shown by red dotted outline).

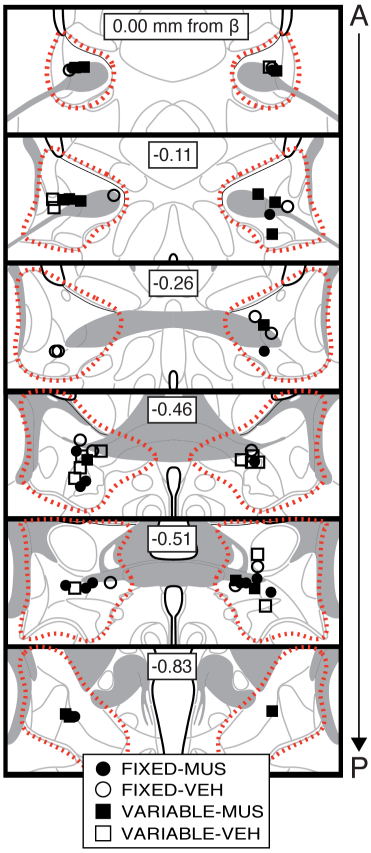

Figure 3—Figure Supplement 1
Bilateral cannula placements for BNST microinfusions. Schematic depicting cannula placements for Figure 3. Symbols (split by each group) correspond to injector tips (approximate borders of BNST are shown by red dotted outline).

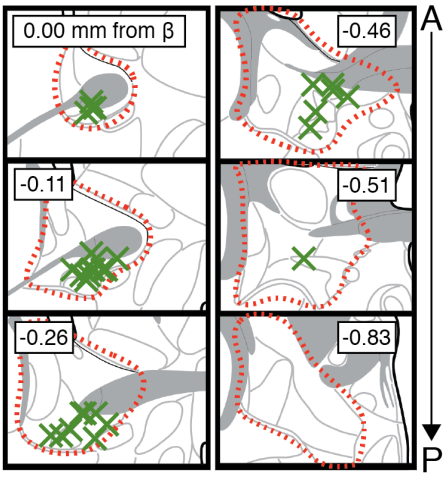

Figure 6—Figure Supplement 1
CTb injection sites in BNST. Approximation of the most ventral and centermost sites of unilateral microinjection of CTb (green X's) for all animals shown in Figure 6 and 7 (red outline approximates borders of BNST).

References

Acca, G.M., Mathew, A.S., Jin, J., Maren, S., Nagaya, N., 2017. Allopregnanolone induces state-dependent fear via the bed nucleus of the stria terminalis. Horm. Behav. 89, 137–144. doi:10.1016/j.yhbeh.2017.01.002

Adami, M.B., Barretto-de-Souza, L., Duarte, J.O., Almeida, J., Crestani, C.C., 2017. Both N-methyl-D-aspartate and non-N-methyl-D-aspartate glutamate receptors in the bed nucleus of the stria terminalis modulate the cardiovascular responses to acute restraint stress in rats. J. Psychopharmacol. (Oxford) 31, 674–681. doi:10.1177/0269881117691468

Alvarez, R.P., Chen, G., Bodurka, J., Kaplan, R., Grillon, C., 2011. Phasic and sustained fear in humans elicits distinct patterns of brain activity. Neuroimage 55, 389–400. doi:10.1016/j.neuroimage.2010.11.057

Alvarez, R.P., Kirlic, N., Misaki, M., Bodurka, J., Rhudy, J.L., Paulus, M.P., Drevets, W.C., 2015. Increased anterior insula activity in anxious individuals is linked to diminished perceived control. Transl. Psychiatry 5, e591. doi:10.1038/tp.2015.84

Amadi, U., Lim, S.H., Liu, E., Baratta, M.V., Goosens, K.A., 2017. Hippocampal processing of ambiguity enhances fear memory. Psychol. Sci. 28, 143–161. doi:10.1177/0956797616674055

Andreatta, M., Fendt, M., Mühlberger, A., Wieser, M.J., Imobersteg, S., Yarali, A., Gerber, B., Pauli, P., 2012. Onset and offset of aversive events establish distinct memories requiring fear and reward networks. Learn. Mem. 19, 518–526. doi:10.1101/lm.026864.112

Andreescu, C., Sheu, L.K., Tudorascu, D., Gross, J.J., Walker, S., Banihashemi, L., Aizenstein, H., 2015. Emotion reactivity and regulation in late-life generalized anxiety disorder: functional connectivity at baseline and post-treatment. Am. J. Geriatr. Psychiatry 23, 200–214. doi:10.1016/j.jagp.2014.05.003

Asok, A., Draper, A., Hoffman, A.F., Schulkin, J., Lupica, C.R., Rosen, J.B., 2018. Optogenetic silencing of a corticotropin-releasing factor pathway from the central amygdala to the bed nucleus of the stria terminalis disrupts sustained fear. Mol. Psychiatry 23, 914–922. doi:10.1038/mp.2017.79

Aston-Jones, G., Harris, G.C., 2004. Brain substrates for increased drug seeking during protracted withdrawal. Neuropharmacology 47 Suppl 1, 167–179. doi:10.1016/j.neuropharm.2004.06.020

Avery, S.N., Clauss, J.A., Blackford, J.U., 2016. The human BNST: functional role in anxiety and addiction. Neuropsychopharmacology 41, 126–141. doi:10.1038/npp.2015.185

Avery, S.N., Clauss, J.A., Winder, D.G., Woodward, N., Heckers, S., Blackford, J.U., 2014. BNST neurocircuitry in humans. Neuroimage 91, 311–323. doi:10.1016/j.neuroimage.2014.01.017

Ayres, J.J.., Mahoney, W.J., Proulx, D.T., Benedict, J.O., 1976. Backward conditioning as an extinction procedure. Learn Motiv 7, 368–381. doi:10.1016/0023-9690(76)90043-6

Ayres, J.J.B., Haddad, C., Albert, M., 1987. One-trial excitatory backward conditioning as assessed by conditioned suppression of licking in rats: Concurrent observations of lick suppression and defensive behaviors. Anim Learn Behav 15, 212–217. doi:10.3758/BF03204964

Bali, A., Jaggi, A.S., 2015. Electric foot shock stress: a useful tool in neuropsychiatric studies. Rev Neurosci 26, 655–677. doi:10.1515/revneuro-2015-0015

Bangasser, D.A., Santollo, J., Shors, T.J., 2005. The bed nucleus of the stria terminalis is

critically involved in enhancing associative learning after stressful experience. Behav. Neurosci. 119, 1459–1466. doi:10.1037/0735-7044.119.6.1459
Barnet, R.C., Miller, R.R., 1996. Second-order excitation mediated by a backward conditioned inhibitor. Journal of Experimental Psychology: Animal Behavior Processes 22, 279–296. doi:10.1037/0097-7403.22.3.279
Behar, E., DiMarco, I.D., Hekler, E.B., Mohlman, J., Staples, A.M., 2009. Current theoretical models of generalized anxiety disorder (GAD): conceptual review and treatment implications. J. Anxiety Disord. 23, 1011–1023. doi:10.1016/j.janxdis.2009.07.006
Bennett, K.P., Dickmann, J.S., Larson, C.L., 2018. If or when? Uncertainty's role in anxious anticipation. Psychophysiology 55, e13066. doi:10.1111/psyp.13066
Berridge, K.C., 2018. Evolving concepts of emotion and motivation. Front. Psychol. 9, 1647. doi:10.3389/fpsyg.2018.01647
Besnard, A., Gao, Y., TaeWoo Kim, M., Twarkowski, H., Reed, A.K., Langberg, T., Feng, W., Xu, X., Saur, D., Zweifel, L.S., Davison, I., Sahay, A., 2019. Dorsolateral septum somatostatin interneurons gate mobility to calibrate context-specific behavioral fear responses. Nat. Neurosci. doi:10.1038/s41593-018-0330-y
Bevins, R.A., Ayres, J.J., 1992. One-trial backward excitatory fear conditioning transfers across contexts. Behav. Res. Ther. 30, 551–554. doi:10.1016/0005-7967(92)90041-E
Blanco, C., Xu, Y., Schneier, F.R., Okuda, M., Liu, S.-M., Heimberg, R.G., 2011. Predictors of persistence of social anxiety disorder: a national study. J. Psychiatr. Res. 45, 1557–1563. doi:10.1016/j.jpsychires.2011.08.004
Breitfeld, T., Bruning, J.E.A., Inagaki, H., Takeuchi, Y., Kiyokawa, Y., Fendt, M., 2015. Temporary inactivation of the anterior part of the bed nucleus of the stria terminalis blocks alarm pheromone-induced defensive behavior in rats. Front. Neurosci. 9, 321. doi:10.3389/fnins.2015.00321
Brinkmann, L., Buff, C., Feldker, K., Neumeister, P., Heitmann, C.Y., Hofmann, D., Bruchmann, M., Herrmann, M.J., Straube, T., 2018. Inter-individual differences in trait anxiety shape the functional connectivity between the bed nucleus of the stria terminalis and the amygdala during brief threat processing. Neuroimage 166, 110–116. doi:10.1016/j.neuroimage.2017.10.054
Brinkmann, L, Buff, C., Feldker, K., Tupak, S.V., Becker, M.P.I., Herrmann, M.J., Straube, T., 2017. Distinct phasic and sustained brain responses and connectivity of amygdala and bed nucleus of the stria terminalis during threat anticipation in panic disorder. Psychol. Med. 47, 2675–2688. doi:10.1017/S0033291717001192
Brinkmann, Leonie, Buff, C., Neumeister, P., Tupak, S.V., Becker, M.P.I., Herrmann, M.J., Straube, T., 2017. Dissociation between amygdala and bed nucleus of the stria terminalis during threat anticipation in female post-traumatic stress disorder patients. Hum. Brain Mapp. 38, 2190–2205. doi:10.1002/hbm.23513
Buff, C., Brinkmann, L., Bruchmann, M., Becker, M.P.I., Tupak, S., Herrmann, M.J., Straube, T., 2017. Activity alterations in the bed nucleus of the stria terminalis and amygdala during threat anticipation in generalized anxiety disorder. Soc. Cogn. Affect. Neurosci. 12, 1766–1774. doi:10.1093/scan/nsx103
Buffalari, D.M., See, R.E., 2011. Inactivation of the bed nucleus of the stria terminalis in an animal model of relapse: effects on conditioned cue-induced reinstatement and its enhancement by yohimbine. Psychopharmacology 213, 19–27. doi:10.1007/s00213-010-2008-3

Burman, M.A., Simmons, C.A., Hughes, M., Lei, L., 2014. Developing and validating trace fear conditioning protocols in C57BL/6 mice. J. Neurosci. Methods 222, 111–117. doi:10.1016/j.jneumeth.2013.11.005

Campeau, S., Falls, W.A., Cullinan, W.E., Helmreich, D.L., Davis, M., Watson, S.J., 1997. Elicitation and reduction of fear: behavioural and neuroendocrine indices and brain induction of the immediate-early gene c-fos. Neuroscience 78, 1087–1104. doi:10.1016/S0306-4522(96)00632-X

Canteras, N.S., Swanson, L.W., 1992. Projections of the ventral subiculum to the amygdala, septum, and hypothalamus: a PHAL anterograde tract-tracing study in the rat. J. Comp. Neurol. 324, 180–194. doi:10.1002/cne.903240204

Chang, R.C., Blaisdell, A.P., Miller, R.R., 2003. Backward conditioning: mediation by the context. J Exp Psychol Anim Behav Process 29, 171–183. doi:10.1037/0097-7403.29.3.171

Ch'ng, S., Fu, J., Brown, R.M., McDougall, S.J., Lawrence, A.J., 2018. The intersection of stress and reward: BNST modulation of aversive and appetitive states. Prog. Neuropsychopharmacol. Biol. Psychiatry 87, 108–125. doi:10.1016/j.pnpbp.2018.01.005

Choi, J.M., Padmala, S., Pessoa, L., 2012. Impact of state anxiety on the interaction between threat monitoring and cognition. Neuroimage 59, 1912–1923. doi:10.1016/j.neuroimage.2011.08.102

Choi, J.M., Padmala, S., Spechler, P., Pessoa, L., 2014. Pervasive competition between threat and reward in the brain. Soc. Cogn. Affect. Neurosci. 9, 737–750. doi:10.1093/scan/nst053

Christianson, J.P., Jennings, J.H., Ragole, T., Flyer, J.G.N., Benison, A.M., Barth, D.S., Watkins, L.R., Maier, S.F., 2011. Safety signals mitigate the consequences of uncontrollable stress via a circuit involving the sensory insular cortex and bed nucleus of the stria terminalis. Biol. Psychiatry 70, 458–464. doi:10.1016/j.biopsych.2011.04.004

Coaster, M., Rogers, B.P., Jones, O.D., Viscusi, W.K., Merkle, K.L., Zald, D.H., Gore, J.C., 2011. Variables influencing the neural correlates of perceived risk of physical harm. Cogn Affect Behav Neurosci 11, 494–507. doi:10.3758/s13415-011-0047-9

Colvonen, P.J., Glassman, L.H., Crocker, L.D., Buttner, M.M., Orff, H., Schiehser, D.M., Norman, S.B., Afari, N., 2017. Pretreatment biomarkers predicting PTSD psychotherapy outcomes: A systematic review. Neurosci. Biobehav. Rev. 75, 140–156. doi:10.1016/j.neubiorev.2017.01.027

Comer, J.S., Blanco, C., Hasin, D.S., Liu, S.-M., Grant, B.F., Turner, J.B., Olfson, M., 2011. Health-related quality of life across the anxiety disorders: results from the national epidemiologic survey on alcohol and related conditions (NESARC). J. Clin. Psychiatry 72, 43–50. doi:10.4088/JCP.09m05094blu

Connor, D.A., Kutlu, M.G., Gould, T.J., 2017. Nicotine disrupts safety learning by enhancing fear associated with a safety cue via the dorsal hippocampus. J. Psychopharmacol. (Oxford) 31, 934–944. doi:10.1177/0269881117695861

Corcoran, K.A., Quirk, G.J., 2007. Activity in prelimbic cortex is necessary for the expression of learned, but not innate, fears. J. Neurosci. 27, 840–844. doi:10.1523/JNEUROSCI.5327-06.2007

Costello, E.J., He, J., Sampson, N.A., Kessler, R.C., Merikangas, K.R., 2014. Services for adolescents with psychiatric disorders: 12-month data from the National Comorbidity Survey-Adolescent. Psychiatr. Serv. 65, 359–366. doi:10.1176/appi.ps.201100518

Crestani, C.C., Alves, F.H., Gomes, F.V., Resstel, L.B., Correa, F.M., Herman, J.P., 2013. Mechanisms in the bed nucleus of the stria terminalis involved in control of autonomic and neuroendocrine functions: a review. Curr Neuropharmacol 11, 141–159. doi:10.2174/1570159X11311020002

Crowley, N.A., Bloodgood, D.W., Hardaway, J.A., Kendra, A.M., McCall, J.G., Al-Hasani, R., McCall, N.M., Yu, W., Schools, Z.L., Krashes, M.J., Lowell, B.B., Whistler, J.L., Bruchas, M.R., Kash, T.L., 2016. Dynorphin controls the gain of an amygdalar anxiety circuit. Cell Rep. 14, 2774–2783. doi:10.1016/j.celrep.2016.02.069

Daldrup, T., Lesting, J., Meuth, P., Seidenbecher, T., Pape, H.-C., 2016. Neuronal correlates of sustained fear in the anterolateral part of the bed nucleus of stria terminalis. Neurobiol. Learn. Mem. 131, 137–146. doi:10.1016/j.nlm.2016.03.020

Daldrup, T., Remmes, J., Lesting, J., Gaburro, S., Fendt, M., Meuth, P., Kloke, V., Pape, H.C., Seidenbecher, T., 2015. Expression of freezing and fear-potentiated startle during sustained fear in mice. Genes Brain Behav. 14, 281–291. doi:10.1111/gbb.12211

Daniel, S.E., Rainnie, D.G., 2016. Stress modulation of opposing circuits in the bed nucleus of the stria terminalis. Neuropsychopharmacology 41, 103–125. doi:10.1038/npp.2015.178

Davies, C.D., Craske, M.G., 2015. Psychophysiological responses to unpredictable threat: effects of cue and temporal unpredictability. Emotion 15, 195–200. doi:10.1037/emo0000038

Davis, M., 2006. Neural systems involved in fear and anxiety measured with fear-potentiated startle. Am. Psychol. 61, 741–756. doi:10.1037/0003-066X.61.8.741

Davis, M., Walker, D.L., 2014. Role of bed nucleus of the stria terminalis and amygdala AMPA receptors in the development and expression of context conditioning and sensitization of startle by prior shock. Brain Struct. Funct. 219, 1969–1982. doi:10.1007/s00429-013-0616-5

Davis, M., Walker, D.L., Miles, L., Grillon, C., 2010. Phasic vs sustained fear in rats and humans: role of the extended amygdala in fear vs anxiety. Neuropsychopharmacology 35, 105–135. doi:10.1038/npp.2009.109

deCampo, D.M., Fudge, J.L., 2013. Amygdala projections to the lateral bed nucleus of the stria terminalis in the macaque: comparison with ventral striatal afferents. J. Comp. Neurol. 521, 3191–3216. doi:10.1002/cne.23340

Deslauriers, J., Toth, M., Der-Avakian, A., Risbrough, V.B., 2017. Current status of animal models of posttraumatic stress disorder: behavioral and biological phenotypes, and future challenges in improving translation. Biol. Psychiatry. doi:10.1016/j.biopsych.2017.11.019

Dong, H.W., Petrovich, G.D., Swanson, L.W., 2001. Topography of projections from amygdala to bed nuclei of the stria terminalis. Brain Res Brain Res Rev 38, 192–246. doi:10.1016/S0165-0173(01)00079-0

Fanselow, M.S., 1994. Neural organization of the defensive behavior system responsible for fear. Psychon. Bull. Rev. 1, 429–438. doi:10.3758/BF03210947

Fanselow, M.S., Pennington, Z.T., 2017. The Danger of LeDoux and Pine's Two-System Framework for Fear. Am. J. Psychiatry 174, 1120–1121. doi:10.1176/appi.ajp.2017.17070818

Fanselow, M.S., Pennington, Z.T., 2018. A return to the psychiatric dark ages with a two-system framework for fear. Behav. Res. Ther. 100, 24–29. doi:10.1016/j.brat.2017.10.012

Fendt, M., Endres, T., Apfelbach, R., 2003. Temporary inactivation of the bed nucleus of the stria terminalis but not of the amygdala blocks freezing induced by trimethylthiazoline, a

component of fox feces. J. Neurosci. 23, 23–28.
Forray, M.I., Gysling, K., 2004. Role of noradrenergic projections to the bed nucleus of the stria terminalis in the regulation of the hypothalamic-pituitary-adrenal axis. Brain Res Brain Res Rev 47, 145–160. doi:10.1016/j.brainresrev.2004.07.011
Fox, A.S., Oler, J.A., Birn, R.M., Shackman, A.J., Alexander, A.L., Kalin, N.H., 2018. Functional Connectivity within the Primate Extended Amygdala Is Heritable and Associated with Early-Life Anxious Temperament. J. Neurosci. 38, 7611–7621. doi:10.1523/JNEUROSCI.0102-18.2018
Fox, A.S., Shackman, A.J., 2017. The central extended amygdala in fear and anxiety: Closing the gap between mechanistic and neuroimaging research. Neurosci. Lett. doi:10.1016/j.neulet.2017.11.056
Fox, A.S., Shelton, S.E., Oakes, T.R., Converse, A.K., Davidson, R.J., Kalin, N.H., 2010. Orbitofrontal cortex lesions alter anxiety-related activity in the primate bed nucleus of stria terminalis. J. Neurosci. 30, 7023–7027. doi:10.1523/JNEUROSCI.5952-09.2010
Gerber, B., Yarali, A., Diegelmann, S., Wotjak, C.T., Pauli, P., Fendt, M., 2014. Pain-relief learning in flies, rats, and man: basic research and applied perspectives. Learn. Mem. 21, 232–252. doi:10.1101/lm.032995.113
Gewirtz, J.C., McNish, K.A., Davis, M., 1998. Lesions of the bed nucleus of the stria terminalis block sensitization of the acoustic startle reflex produced by repeated stress, but not fear-potentiated startle. Prog. Neuropsychopharmacol. Biol. Psychiatry 22, 625–648.
Glangetas, C., Girard, D., Groc, L., Marsicano, G., Chaouloff, F., Georges, F., 2013. Stress switches cannabinoid type-1 (CB1) receptor-dependent plasticity from LTD to LTP in the bed nucleus of the stria terminalis. J. Neurosci. 33, 19657–19663. doi:10.1523/JNEUROSCI.3175-13.2013
Glangetas, C., Massi, L., Fois, G.R., Jalabert, M., Girard, D., Diana, M., Yonehara, K., Roska, B., Xu, C., Lüthi, A., Caille, S., Georges, F., 2017. NMDA-receptor-dependent plasticity in the bed nucleus of the stria terminalis triggers long-term anxiolysis. Nat. Commun. 8, 14456. doi:10.1038/ncomms14456
Goode, T.D., Jin, J., Maren, S., 2018. Neural circuits for fear relapse, in: Neurobiology of Abnormal Emotion and Motivated Behaviors. Academic Press.
Goode, T.D., Kim, J.J., Maren, S., 2015. Reversible inactivation of the bed nucleus of the stria terminalis prevents reinstatement but not renewal of extinguished fear. Eneuro 2. doi:10.1523/ENEURO.0037-15.2015
Goode, T.D., Maren, S., 2017. Role of the bed nucleus of the stria terminalis in aversive learning and memory. Learn. Mem. 24, 480–491. doi:10.1101/lm.044206.116
Goode, T.D., Maren, S., 2018. Common neurocircuitry mediating drug and fear relapse in preclinical models. Psychopharmacology. doi:10.1007/s00213-018-5024-3
Graham, B.M., Callaghan, B.L., Richardson, R., 2014. Bridging the gap: Lessons we have learnt from the merging of psychology and psychiatry for the optimisation of treatments for emotional disorders. Behav. Res. Ther. 62, 3–16. doi:10.1016/j.brat.2014.07.012
Grupe, D.W., Oathes, D.J., Nitschke, J.B., 2013. Dissecting the anticipation of aversion reveals dissociable neural networks. Cereb. Cortex 23, 1874–1883. doi:10.1093/cercor/bhs175
Gungor, N.Z., Paré, D., 2016. Functional heterogeneity in the bed nucleus of the stria terminalis. J. Neurosci. 36, 8038–8049. doi:10.1523/JNEUROSCI.0856-16.2016
Hammack, S.E., Guo, J.-D., Hazra, R., Dabrowska, J., Myers, K.M., Rainnie, D.G., 2009. The response of neurons in the bed nucleus of the stria terminalis to serotonin: implications

for anxiety. Prog. Neuropsychopharmacol. Biol. Psychiatry 33, 1309–1320. doi:10.1016/j.pnpbp.2009.05.013
Hammack, S.E., Todd, T.P., Kocho-Schellenberg, M., Bouton, M.E., 2015. Role of the bed nucleus of the stria terminalis in the acquisition of contextual fear at long or short context-shock intervals. Behav. Neurosci. 129, 673–678. doi:10.1037/bne0000088
Harris, N.A., Winder, D.G., 2018. Synaptic Plasticity in the Bed Nucleus of the Stria Terminalis: Underlying Mechanisms and Potential Ramifications for Reinstatement of Drug- and Alcohol-Seeking Behaviors. ACS Chem. Neurosci. 9, 2173–2187. doi:10.1021/acschemneuro.8b00169
Haufler, D., Nagy, F.Z., Pare, D., 2013. Neuronal correlates of fear conditioning in the bed nucleus of the stria terminalis. Learn. Mem. 20, 633–641. doi:10.1101/lm.031799.113
Herrmann, M.J., Boehme, S., Becker, M.P.I., Tupak, S.V., Guhn, A., Schmidt, B., Brinkmann, L., Straube, T., 2016. Phasic and sustained brain responses in the amygdala and the bed nucleus of the stria terminalis during threat anticipation. Hum. Brain Mapp. 37, 1091–1102. doi:10.1002/hbm.23088
Herry, C., Ciocchi, S., Senn, V., Demmou, L., Müller, C., Lüthi, A., 2008. Switching on and off fear by distinct neuronal circuits. Nature 454, 600–606. doi:10.1038/nature07166
Heth, C.D., 1976. Simultaneous and backward fear conditioning as a function of number of CS-UCS pairings. Journal of Experimental Psychology: Animal Behavior Processes 2, 117–129. doi:10.1037/0097-7403.2.2.117
Iza, M., Olfson, M., Vermes, D., Hoffer, M., Wang, S., Blanco, C., 2013. Probability and predictors of first treatment contact for anxiety disorders in the United States: analysis of data from the National Epidemiologic Survey on Alcohol and Related Conditions (NESARC). J. Clin. Psychiatry 74, 1093–1100. doi:10.4088/JCP.13m08361
Jennings, J.H., Sparta, D.R., Stamatakis, A.M., Ung, R.L., Pleil, K.E., Kash, T.L., Stuber, G.D., 2013. Distinct extended amygdala circuits for divergent motivational states. Nature 496, 224–228. doi:10.1038/nature12041
Jin, J., Maren, S., 2015. Fear renewal preferentially activates ventral hippocampal neurons projecting to both amygdala and prefrontal cortex in rats. Sci. Rep. 5, 8388. doi:10.1038/srep08388
Johnson, S.B., Emmons, E.B., Lingg, R.T., Anderson, R.M., Romig-Martin, S.A., LaLumiere, R.T., Narayanan, N.S., Viau, V., Radley, J.J., 2018. Prefrontal-bed nucleus circuit modulation of a passive coping response set. J. Neurosci. doi:10.1523/JNEUROSCI.1421-18.2018
Kalin, N.H., Shelton, S.E., Fox, A.S., Oakes, T.R., Davidson, R.J., 2005. Brain regions associated with the expression and contextual regulation of anxiety in primates. Biol. Psychiatry 58, 796–804. doi:10.1016/j.biopsych.2005.05.021
Kalin, N.H., Shelton, S.E., Fox, A.S., Rogers, J., Oakes, T.R., Davidson, R.J., 2008. The serotonin transporter genotype is associated with intermediate brain phenotypes that depend on the context of eliciting stressor. Mol. Psychiatry 13, 1021–1027. doi:10.1038/mp.2008.37
Kim, S.-Y., Adhikari, A., Lee, S.Y., Marshel, J.H., Kim, C.K., Mallory, C.S., Lo, M., Pak, S., Mattis, J., Lim, B.K., Malenka, R.C., Warden, M.R., Neve, R., Tye, K.M., Deisseroth, K., 2013. Diverging neural pathways assemble a behavioural state from separable features in anxiety. Nature 496, 219–223. doi:10.1038/nature12018
Kinley, D.J., Walker, J.R., Enns, M.W., Sareen, J., 2011. Panic attacks as a risk for later

psychopathology: results from a nationally representative survey. Depress. Anxiety 28, 412–419. doi:10.1002/da.20809
Kinnison, J., Padmala, S., Choi, J.-M., Pessoa, L., 2012. Network analysis reveals increased integration during emotional and motivational processing. J. Neurosci. 32, 8361–8372. doi:10.1523/JNEUROSCI.0821-12.2012
Kiyokawa, Y., Mikami, K., Mikamura, Y., Ishii, A., Takeuchi, Y., Mori, Y., 2015. The 3-second auditory conditioned stimulus is a more effective stressor than the 20-second auditory conditioned stimulus in male rats. Neuroscience 299, 79–87. doi:10.1016/j.neuroscience.2015.04.055
Klumpers, F., Kroes, M.C., Heitland, I., Everaerd, D., Akkermans, S.E.A., Oosting, R.S., van Wingen, G., Franke, B., Kenemans, J.L., Fernández, G., Baas, J.M.P., 2015. Dorsomedial prefrontal cortex mediates the impact of serotonin transporter linked polymorphic region genotype on anticipatory threat reactions. Biol. Psychiatry 78, 582–589. doi:10.1016/j.biopsych.2014.07.034
Klumpers, F., Kroes, M.C.W., Baas, J.M.P., Fernández, G., 2017. How human amygdala and bed nucleus of the stria terminalis may drive distinct defensive responses. J. Neurosci. 37, 9645–9656. doi:10.1523/JNEUROSCI.3830-16.2017
Knapska, E., Maren, S., 2009. Reciprocal patterns of c-Fos expression in the medial prefrontal cortex and amygdala after extinction and renewal of conditioned fear. Learn. Mem. 16, 486–493. doi:10.1101/lm.1463909
Kunwar, P.S., Zelikowsky, M., Remedios, R., Cai, H., Yilmaz, M., Meister, M., Anderson, D.J., 2015. Ventromedial hypothalamic neurons control a defensive emotion state. Elife 4. doi:10.7554/eLife.06633
Lange, M.D., Daldrup, T., Remmers, F., Szkudlarek, H.J., Lesting, J., Guggenhuber, S., Ruehle, S., Jüngling, K., Seidenbecher, T., Lutz, B., Pape, H.C., 2017. Cannabinoid CB1 receptors in distinct circuits of the extended amygdala determine fear responsiveness to unpredictable threat. Mol. Psychiatry 22, 1422–1430. doi:10.1038/mp.2016.156
Lebow, M.A., Chen, A., 2016. Overshadowed by the amygdala: the bed nucleus of the stria terminalis emerges as key to psychiatric disorders. Mol. Psychiatry 21, 450–463. doi:10.1038/mp.2016.1
LeDoux, J., Daw, N.D., 2018. Surviving threats: neural circuit and computational implications of a new taxonomy of defensive behaviour. Nat. Rev. Neurosci. 19, 269–282. doi:10.1038/nrn.2018.22
LeDoux, J.E., Iwata, J., Cicchetti, P., Reis, D.J., 1988. Different projections of the central amygdaloid nucleus mediate autonomic and behavioral correlates of conditioned fear. J. Neurosci. 8, 2517–2529.
Lemos, J.I., Resstel, L.B., Guimarães, F.S., 2010. Involvement of the prelimbic prefrontal cortex on cannabidiol-induced attenuation of contextual conditioned fear in rats. Behav. Brain Res. 207, 105–111. doi:10.1016/j.bbr.2009.09.045
Luyck, K., Goode, T.D., Lee Masson, H., Luyten, L., 2018a. Distinct Activity Patterns of the Human Bed Nucleus of the Stria Terminalis and Amygdala during Fear Learning. Neuropsychol Rev. doi:10.1007/s11065-018-9383-7
Luyck, K., Nuttin, B., Luyten, L., 2018b. Electrolytic post-training lesions of the bed nucleus of the stria terminalis block startle potentiation in a cued fear conditioning procedure. Brain Struct. Funct. 223, 1839–1848. doi:10.1007/s00429-017-1591-z
Luyten, L., Casteels, C., Vansteenwegen, D., van Kuyck, K., Koole, M., Van Laere, K., Nuttin,

B., 2012. Micro-positron emission tomography imaging of rat brain metabolism during expression of contextual conditioning. J. Neurosci. 32, 254–263. doi:10.1523/JNEUROSCI.3701-11.2012
Luyten, L., van Kuyck, K., Vansteenwegen, D., Nuttin, B., 2011. Electrolytic lesions of the bed nucleus of the stria terminalis disrupt freezing and startle potentiation in a conditioned context. Behav. Brain Res. 222, 357–362. doi:10.1016/j.bbr.2011.03.066
Mahoney, W.J., Ayres, J.J.B., 1976. One-trial simultaneous and backward fear conditioning as reflected in conditioned suppression of licking in rats. Anim Learn Behav 4, 357–362. doi:10.3758/BF03214421
Marchand, A.R., Luck, D., Di Scala, G., 2004. Trace fear conditioning: a role for context? Arch Ital Biol 142, 251–263.
Marcinkiewcz, C.A., Mazzone, C.M., D'Agostino, G., Halladay, L.R., Hardaway, J.A., DiBerto, J.F., Navarro, M., Burnham, N., Cristiano, C., Dorrier, C.E., Tipton, G.J., Ramakrishnan, C., Kozicz, T., Deisseroth, K., Thiele, T.E., McElligott, Z.A., Holmes, A., Heisler, L.K., Kash, T.L., 2016. Serotonin engages an anxiety and fear-promoting circuit in the extended amygdala. Nature 537, 97–101. doi:10.1038/nature19318
Marek, R., Jin, J., Goode, T.D., Giustino, T.F., Wang, Q., Acca, G.M., Holehonnur, R., Ploski, J.E., Fitzgerald, P.J., Lynagh, T., Lynch, J.W., Maren, S., Sah, P., 2018. Hippocampus-driven feed-forward inhibition of the prefrontal cortex mediates relapse of extinguished fear. Nat. Neurosci. 21, 384–392. doi:10.1038/s41593-018-0073-9
Maren, S., 1998. Overtraining does not mitigate contextual fear conditioning deficits produced by neurotoxic lesions of the basolateral amygdala. J. Neurosci. 18, 3088–3097.
Markham, C.M., Norvelle, A., Huhman, K.L., 2009. Role of the bed nucleus of the stria terminalis in the acquisition and expression of conditioned defeat in Syrian hamsters. Behav. Brain Res. 198, 69–73. doi:10.1016/j.bbr.2008.10.022
McDonald, A.J., Shammah-Lagnado, S.J., Shi, C., Davis, M., 1999. Cortical afferents to the extended amygdala. Ann. N. Y. Acad. Sci. 877, 309–338. doi:10.1111/j.1749-6632.1999.tb09275.x
McHugh, S.B., Barkus, C., Lima, J., Glover, L.R., Sharp, T., Bannerman, D.M., 2015. SERT and uncertainty: serotonin transporter expression influences information processing biases for ambiguous aversive cues in mice. Genes Brain Behav. 14, 330–336. doi:10.1111/gbb.12215
McMenamin, B.W., Langeslag, S.J.E., Sirbu, M., Padmala, S., Pessoa, L., 2014. Network organization unfolds over time during periods of anxious anticipation. J. Neurosci. 34, 11261–11273. doi:10.1523/JNEUROSCI.1579-14.2014
McNally, G.P., Johansen, J.P., Blair, H.T., 2011. Placing prediction into the fear circuit. Trends Neurosci. 34, 283–292. doi:10.1016/j.tins.2011.03.005
Meyer, C., Padmala, S., Pessoa, L., 2018. Dynamic Threat Processing. J. Cogn. Neurosci. 1–21. doi:10.1162/jocn_a_01363
Milad, M.R., Quirk, G.J., 2002. Neurons in medial prefrontal cortex signal memory for fear extinction. Nature 420, 70–74. doi:10.1038/nature01138
Miles, O.W., May, V., Hammack, S.E., 2018. Pituitary Adenylate Cyclase-Activating Peptide (PACAP) Signaling and the Dark Side of Addiction. J. Mol. Neurosci. doi:10.1007/s12031-018-1147-6
Mobbs, D., Yu, R., Rowe, J.B., Eich, H., FeldmanHall, O., Dalgleish, T., 2010. Neural activity associated with monitoring the oscillating threat value of a tarantula. Proc. Natl. Acad.

Sci. USA 107, 20582–20586. doi:10.1073/pnas.1009076107
Moscovitch, A., LoLordo, V.M., 1968. Role of safety in the Pavlovian backward fear conditioning procedure. J Comp Physiol Psychol 66, 673–678. doi:10.1037/h0026548
Motzkin, J.C., Philippi, C.L., Oler, J.A., Kalin, N.H., Baskaya, M.K., Koenigs, M., 2015. Ventromedial prefrontal cortex damage alters resting blood flow to the bed nucleus of stria terminalis. Cortex 64, 281–288. doi:10.1016/j.cortex.2014.11.013
Münsterkötter, A.L., Notzon, S., Redlich, R., Grotegerd, D., Dohm, K., Arolt, V., Kugel, H., Zwanzger, P., Dannlowski, U., 2015. Spider or no spider? neural correlates of sustained and phasic fear in spider phobia. Depress. Anxiety 32, 656–663. doi:10.1002/da.22382
Naaz, F., Knight, L.K., Depue, B.E., 2019. Explicit and ambiguous threat processing: functionally dissociable roles of the amygdala and bed nucleus of the stria terminalis. J. Cogn. Neurosci. 1–17. doi:10.1162/jocn_a_01369
Nagaya, N., Acca, G.M., Maren, S., 2015. Allopregnanolone in the bed nucleus of the stria terminalis modulates contextual fear in rats. Front. Behav. Neurosci. 9, 205. doi:10.3389/fnbeh.2015.00205
Nees, F., Heinrich, A., Flor, H., 2015. A mechanism-oriented approach to psychopathology: The role of Pavlovian conditioning. Int. J. Psychophysiol. 98, 351–364. doi:10.1016/j.ijpsycho.2015.05.005
Orsini, C.A., Kim, J.H., Knapska, E., Maren, S., 2011. Hippocampal and prefrontal projections to the basal amygdala mediate contextual regulation of fear after extinction. J. Neurosci. 31, 17269–17277. doi:10.1523/JNEUROSCI.4095-11.2011
Pedersen, W.S., Balderston, N.L., Miskovich, T.A., Belleau, E.L., Helmstetter, F.J., Larson, C.L., 2017. The effects of stimulus novelty and negativity on BOLD activity in the amygdala, hippocampus, and bed nucleus of the stria terminalis. Soc. Cogn. Affect. Neurosci. 12, 748–757. doi:10.1093/scan/nsw178
Pedersen, W.S., Muftuler, L.T., Larson, C.L., 2018. Conservatism and the neural circuitry of threat: economic conservatism predicts greater amygdala-BNST connectivity during periods of threat vs safety. Soc. Cogn. Affect. Neurosci. 13, 43–51. doi:10.1093/scan/nsx133
Perusini, J.N., Fanselow, M.S., 2015. Neurobehavioral perspectives on the distinction between fear and anxiety. Learn. Mem. 22, 417–425. doi:10.1101/lm.039180.115
Pina, M.M., Young, E.A., Ryabinin, A.E., Cunningham, C.L., 2015. The bed nucleus of the stria terminalis regulates ethanol-seeking behavior in mice. Neuropharmacology 99, 627–638. doi:10.1016/j.neuropharm.2015.08.033
Pine, D.S., LeDoux, J.E., 2017. Elevating the role of subjective experience in the clinic: response to fanselow and pennington. Am. J. Psychiatry 174, 1121–1122. doi:10.1176/appi.ajp.2017.17070818r
Poulos, A.M., Ponnusamy, R., Dong, H.-W., Fanselow, M.S., 2010. Compensation in the neural circuitry of fear conditioning awakens learning circuits in the bed nuclei of the stria terminalis. Proc. Natl. Acad. Sci. USA 107, 14881–14886. doi:10.1073/pnas.1005754107
Prével, A., Rivière, V., Darcheville, J.-C., Urcelay, G.P., 2016. Conditioned reinforcement and backward association. Learn Motiv 56, 38–47. doi:10.1016/j.lmot.2016.09.004
Prével, A., Rivière, V., Darcheville, J.-C., Urcelay, G.P., Miller, R.R., 2018. Excitatory second-order conditioning using a backward first-order conditioned stimulus: A challenge for prediction error reduction. Q J Exp Psychol (Colchester) 1747021818793376. doi:10.1177/1747021818793376

Quirk, G.J., Mueller, D., 2008. Neural mechanisms of extinction learning and retrieval. Neuropsychopharmacology 33, 56–72. doi:10.1038/sj.npp.1301555
Rabellino, D., Densmore, M., Harricharan, S., Jean, T., McKinnon, M.C., Lanius, R.A., 2018. Resting-state functional connectivity of the bed nucleus of the stria terminalis in post-traumatic stress disorder and its dissociative subtype. Hum. Brain Mapp. 39, 1367–1379. doi:10.1002/hbm.23925
Radley, J.J., Gosselink, K.L., Sawchenko, P.E., 2009. A discrete GABAergic relay mediates medial prefrontal cortical inhibition of the neuroendocrine stress response. J. Neurosci. 29, 7330–7340. doi:10.1523/JNEUROSCI.5924-08.2009
Radley, J.J., Johnson, S.B., 2018. Anteroventral bed nuclei of the stria terminalis neurocircuitry: Towards an integration of HPA axis modulation with coping behaviors - Curt Richter Award Paper 2017. Psychoneuroendocrinology 89, 239–249. doi:10.1016/j.psyneuen.2017.12.005
Radley, J.J., Sawchenko, P.E., 2011. A common substrate for prefrontal and hippocampal inhibition of the neuroendocrine stress response. J. Neurosci. 31, 9683–9695. doi:10.1523/JNEUROSCI.6040-10.2011
Raybuck, J.D., Lattal, K.M., 2014. Bridging the interval: theory and neurobiology of trace conditioning. Behav. Processes 101, 103–111. doi:10.1016/j.beproc.2013.08.016
Reichard, R.A., Subramanian, S., Desta, M.T., Sura, T., Becker, M.L., Ghobadi, C.W., Parsley, K.P., Zahm, D.S., 2017. Abundant collateralization of temporal lobe projections to the accumbens, bed nucleus of stria terminalis, central amygdala and lateral septum. Brain Struct. Funct. 222, 1971–1988. doi:10.1007/s00429-016-1321-y
Rescorla, R.A., 1968. Probability of shock in the presence and absence of CS in fear conditioning. J Comp Physiol Psychol 66, 1–5. doi:10.1037/h0025984
Reynolds, S.M., Zahm, D.S., 2005. Specificity in the projections of prefrontal and insular cortex to ventral striatopallidum and the extended amygdala. J. Neurosci. 25, 11757–11767. doi:10.1523/JNEUROSCI.3432-05.2005
Sajdyk, T., Johnson, P., Fitz, S., Shekhar, A., 2008. Chronic inhibition of GABA synthesis in the bed nucleus of the stria terminalis elicits anxiety-like behavior. J. Psychopharmacol. (Oxford) 22, 633–641. doi:10.1177/0269881107082902
Salas-Wright, C.P., Kagotho, N., Vaughn, M.G., 2014. Mood, anxiety, and personality disorders among first and second-generation immigrants to the United States. Psychiatry Res. 220, 1028–1036. doi:10.1016/j.psychres.2014.08.045
Sangha, S., Robinson, P.D., Greba, Q., Davies, D.A., Howland, J.G., 2014. Alterations in reward, fear and safety cue discrimination after inactivation of the rat prelimbic and infralimbic cortices. Neuropsychopharmacology 39, 2405–2413. doi:10.1038/npp.2014.89
Schlund, M.W., Hudgins, C.D., Magee, S., Dymond, S., 2013. Neuroimaging the temporal dynamics of human avoidance to sustained threat. Behav. Brain Res. 257, 148–155. doi:10.1016/j.bbr.2013.09.042
Schneider, C.A., Rasband, W.S., Eliceiri, K.W., 2012. NIH Image to ImageJ: 25 years of image analysis. Nat. Methods 9, 671–675.
Schroijen, M., Fantoni, S., Rivera, C., Vervliet, B., Schruers, K., van den Bergh, O., van Diest, I., 2016. Defensive activation to (un)predictable interoceptive threat: The NPU respiratory threat test (NPUr). Psychophysiology 53, 905–913. doi:10.1111/psyp.12621
Seidenbecher, T., Remmes, J., Daldrup, T., Lesting, J., Pape, H.-C., 2016. Distinct state anxiety

after predictable and unpredictable fear training in mice. Behav. Brain Res. 304, 20–23. doi:10.1016/j.bbr.2016.02.009
Shackman, A.J., Fox, A.S., 2016. Contributions of the central extended amygdala to fear and anxiety. J. Neurosci. 36, 8050–8063. doi:10.1523/JNEUROSCI.0982-16.2016
Shankman, S.A., Robison-Andrew, E.J., Nelson, B.D., Altman, S.E., Campbell, M.L., 2011. Effects of predictability of shock timing and intensity on aversive responses. Int. J. Psychophysiol. 80, 112–118. doi:10.1016/j.ijpsycho.2011.02.008
Siegel, S., Domjan, M., 1971. Backward conditoning as an inhibitory procedure. Learn Motiv 2, 1–11. doi:10.1016/0023-9690(71)90043-9
Silberman, Y., Winder, D.G., 2013. Emerging role for corticotropin releasing factor signaling in the bed nucleus of the stria terminalis at the intersection of stress and reward. Front. Psychiatry 4, 42. doi:10.3389/fpsyt.2013.00042
Sinnema, H., Majo, M.C., Volker, D., Hoogendoorn, A., Terluin, B., Wensing, M., van Balkom, A., 2015. Effectiveness of a tailored implementation programme to improve recognition, diagnosis and treatment of anxiety and depression in general practice: a cluster randomised controlled trial. Implement. Sci. 10, 33. doi:10.1186/s13012-015-0210-8
Sladky, R., Geissberger, N., Pfabigan, D.M., Kraus, C., Tik, M., Woletz, M., Paul, K., Vanicek, T., Auer, B., Kranz, G.S., Lamm, C., Lanzenberger, R., Windischberger, C., 2018. Unsmoothed functional MRI of the human amygdala and bed nucleus of the stria terminalis during processing of emotional faces. Neuroimage 168, 383–391. doi:10.1016/j.neuroimage.2016.12.024
Somerville, L.H., Whalen, P.J., Kelley, W.M., 2010. Human bed nucleus of the stria terminalis indexes hypervigilant threat monitoring. Biol. Psychiatry 68, 416–424. doi:10.1016/j.biopsych.2010.04.002
Stamatakis, A.M., Sparta, D.R., Jennings, J.H., McElligott, Z.A., Decot, H., Stuber, G.D., 2014. Amygdala and bed nucleus of the stria terminalis circuitry: Implications for addiction-related behaviors. Neuropharmacology 76 Pt B, 320–328. doi:10.1016/j.neuropharm.2013.05.046
Stein, D.J., Scott, K.M., de Jonge, P., Kessler, R.C., 2017. Epidemiology of anxiety disorders: from surveys to nosology and back. Dialogues Clin Neurosci 19, 127–136.
Sterrenburg, L., Gaszner, B., Boerrigter, J., Santbergen, L., Bramini, M., Roubos, E.W., Peeters, B.W.M.M., Kozicz, T., 2012. Sex-dependent and differential responses to acute restraint stress of corticotropin-releasing factor-producing neurons in the rat paraventricular nucleus, central amygdala, and bed nucleus of the stria terminalis. J. Neurosci. Res. 90, 179–192. doi:10.1002/jnr.22737
Straube, T., Mentzel, H.-J., Miltner, W.H.R., 2007. Waiting for spiders: brain activation during anticipatory anxiety in spider phobics. Neuroimage 37, 1427–1436. doi:10.1016/j.neuroimage.2007.06.023
Sullivan, G.M., Apergis, J., Bush, D.E.A., Johnson, L.R., Hou, M., Ledoux, J.E., 2004. Lesions in the bed nucleus of the stria terminalis disrupt corticosterone and freezing responses elicited by a contextual but not by a specific cue-conditioned fear stimulus. Neuroscience 128, 7–14. doi:10.1016/j.neuroscience.2004.06.015
Swanson, L., 2003. Brain Maps, Third Edition: Structure of the Rat Brain (Vol 3), 3rd ed. Academic Press.
Takahashi, L.K., 2014. Olfactory systems and neural circuits that modulate predator odor fear. Front. Behav. Neurosci. 8, 72. doi:10.3389/fnbeh.2014.00072

Tipps, M.E., Raybuck, J.D., Buck, K.J., Lattal, K.M., 2014. Delay and trace fear conditioning in C57BL/6 and DBA/2 mice: issues of measurement and performance. Learn. Mem. 21, 380–393. doi:10.1101/lm.035261.114

Torrisi, S., Gorka, A.X., Gonzalez-Castillo, J., O'Connell, K., Balderston, N., Grillon, C., Ernst, M., 2018. Extended amygdala connectivity changes during sustained shock anticipation. Transl. Psychiatry 8, 33. doi:10.1038/s41398-017-0074-6

Torrisi, S., O'Connell, K., Davis, A., Reynolds, R., Balderston, N., Fudge, J.L., Grillon, C., Ernst, M., 2015. Resting state connectivity of the bed nucleus of the stria terminalis at ultra-high field. Hum. Brain Mapp. 36, 4076–4088. doi:10.1002/hbm.22899

Tye, K.M., 2018. Neural circuit motifs in valence processing. Neuron 100, 436–452. doi:10.1016/j.neuron.2018.10.001

Verma, D., Tasan, R., Sperk, G., Pape, H.-C., 2018. Neuropeptide Y2 receptors in anteroventral BNST control remote fear memory depending on extinction training. Neurobiol. Learn. Mem. 149, 144–153. doi:10.1016/j.nlm.2018.01.011

Vertes, R.P., 2004. Differential projections of the infralimbic and prelimbic cortex in the rat. Synapse 51, 32–58. doi:10.1002/syn.10279

Waddell, J., Bouton, M.E., Falls, W.A., 2008. Central CRF receptor antagonist a-helical CRF9-41 blocks reinstatement of extinguished fear: the role of the bed nucleus of the stria terminalis. Behav. Neurosci. 122, 1061–1069. doi:10.1037/a0013136

Waddell, J., Morris, R.W., Bouton, M.E., 2006. Effects of bed nucleus of the stria terminalis lesions on conditioned anxiety: aversive conditioning with long-duration conditional stimuli and reinstatement of extinguished fear. Behav. Neurosci. 120, 324–336. doi:10.1037/0735-7044.120.2.324

Walker, D.L., Davis, M., 2008. Role of the extended amygdala in short-duration versus sustained fear: a tribute to Dr. Lennart Heimer. Brain Struct. Funct. 213, 29–42. doi:10.1007/s00429-008-0183-3

Walker, D.L., Miles, L.A., Davis, M., 2009. Selective participation of the bed nucleus of the stria terminalis and CRF in sustained anxiety-like versus phasic fear-like responses. Prog. Neuropsychopharmacol. Biol. Psychiatry 33, 1291–1308. doi:10.1016/j.pnpbp.2009.06.022

Wang, Q., Jin, J., Maren, S., 2016. Renewal of extinguished fear activates ventral hippocampal neurons projecting to the prelimbic and infralimbic cortices in rats. Neurobiol. Learn. Mem. 134 Pt A, 38–43. doi:10.1016/j.nlm.2016.04.002

Weller, K.L., Smith, D.A., 1982. Afferent connections to the bed nucleus of the stria terminalis. Brain Res. 232, 255–270. doi:10.1016/0006-8993(82)90272-4

Wittchen, H.-U., 2002. Generalized anxiety disorder: prevalence, burden, and cost to society. Depress. Anxiety 16, 162–171. doi:10.1002/da.10065

Wood, M., Adil, O., Wallace, T., Fourman, S., Wilson, S.P., Herman, J.P., Myers, B., 2018. Infralimbic prefrontal cortex structural and functional connectivity with the limbic forebrain: a combined viral genetic and optogenetic analysis. Brain Struct. Funct. doi:10.1007/s00429-018-1762-6

Xu, H.Y., Liu, Y.J., Xu, M.Y., Zhang, Y.H., Zhang, J.X., Wu, Y.J., 2012. Inactivation of the bed nucleus of the stria terminalis suppresses the innate fear responses of rats induced by the odor of cat urine. Neuroscience 221, 21–27. doi:10.1016/j.neuroscience.2012.06.056

Yassa, M.A., Hazlett, R.L., Stark, C.E.L., Hoehn-Saric, R., 2012. Functional MRI of the amygdala and bed nucleus of the stria terminalis during conditions of uncertainty in

generalized anxiety disorder. J. Psychiatr. Res. 46, 1045–1052. doi:10.1016/j.jpsychires.2012.04.013

Zelikowsky, M., Bissiere, S., Hast, T.A., Bennett, R.Z., Abdipranoto, A., Vissel, B., Fanselow, M.S., 2013. Prefrontal microcircuit underlies contextual learning after hippocampal loss. Proc. Natl. Acad. Sci. USA 110, 9938–9943. doi:10.1073/pnas.1301691110

Zelikowsky, M., Hui, M., Karigo, T., Choe, A., Yang, B., Blanco, M.R., Beadle, K., Gradinaru, V., Deverman, B.E., Anderson, D.J., 2018. The neuropeptide tac2 controls a distributed brain state induced by chronic social isolation stress. Cell 173, 1265–1279.e19. doi:10.1016/j.cell.2018.03.037

Zhu, W., Umegaki, H., Suzuki, Y., Miura, H., Iguchi, A., 2001. Involvement of the bed nucleus of the stria terminalis in hippocampal cholinergic system-mediated activation of the hypothalamo--pituitary--adrenocortical axis in rats. Brain Res. 916, 101–106.

Zimmerman, J.M., Maren, S., 2011. The bed nucleus of the stria terminalis is required for the expression of contextual but not auditory freezing in rats with basolateral amygdala lesions. Neurobiol. Learn. Mem. 95, 199–205. doi:10.1016/j.nlm.2010.11.002